DOKUZ EYLÜL UNIVERSITY

GRADUATE SCHOOL OF NATURAL AND APPLIED SCIENCES

STRUCTURAL AND TEXTURAL FEATURES OF THE KAVACIK GRANITE IN BORNOVA MELANGE

by

Reyhan PEŞTEMALCI ÜREGEL

September, 2019

İZMİR

STRUCTURAL AND TEXTURAL FEATURES OF THE KAVACIK GRANITE IN BORNOVA MELANGE

A Thesis Submitted to the
Graduate School of Natural and Applied Sciences of Dokuz Eylül University
In Partial Fulfillment of the Requirements for the Degree of Master of Science in Geological Engineering, Applied Geology Program

by

Reyhan PEŞTEMALCI ÜREGEL

September, 2019

İZMİR

M.Sc THESIS EXAMINATION RESULT FORM

We have read the thesis entitled **"STRUCTURAL AND TEXTURAL FEATURES OF THE KAVACIK GRANITE IN BORNOVA MELANGE"** completed by **REYHAN PEŞTEMALCI ÜREGEL** under supervision of **PROF. DR. TALİP GÜNGÖR** and we certify that in our opinion it is fully adequate, in scope and in quality, as a thesis for the degree of Master of Science.

....
Prof. Dr. Talip GÜNGÖR

Supervisor

Prof. Dr. Suhan ÖZDEN

(Jury Member)

Doç. Dr. Altuğ HASÖZBEK

(Jury Member)

Prof.Dr. Kadriye ERTEKİN
Director
Graduate School of Natural and Applied Sciences

ACKNOWLEDGEMENTS

I would like to express my appreciation to Prof. Dr. Talip GÜNGÖR for his kind supervision and insightful comments throughout the study. Discussion with Assoc. Prof. Dr. Cüneyt Akal and Dr. Altuğ Hasözbek are gratefully acknowledged. This study was financially supported by Department of Scientific Research Projects of Dokuz Eylül University, Izmir (Project no: 20116.KB.FBE.044). I thank Özge GÜMÜŞ, Sevim KILIÇ, Fırat AKINCI, Ulaş ÇAYBAŞI and Aşkın KÜÇÜKER at Department of Scientific Research Projects.

Reyhan PEŞTEMALCI ÜREGEL

STRUCTURAL AND TEXTURAL FEATURES OF THE KAVACIK GRANITE IN BORNOVA MELANGE

ABSTRACT

The Bornova melange comprises an olistostrome-melange situated NE-SW direction between the Izmir Ankara Suture Zone and the Menderes Massif. The Bornova melange is mainly composed of strongly deformed Late Cretaceous to Late Paleocene sandstone and shale matrix with huge blocks of Mesozoic platform limestone and oceanic crustal associations as tectonic slices. These large-scale limestone blocks in the matrix of the Bornova melange are mostly defined as limestone, basalt, serpentinite and radiolarian cherts. In this study, granitic tectonic slice situated in the Bornova melange named as Kavacık tectonic slice is examined for the first time, in terms of its geological features and its U-Pb zircon crystallization ages. The intrusive boundary relation of the Kavacık granitoid is not clear in the field and displays tectonic boundary with the other tectonics slices. Kavacık tectonic slice displays a typical granitic texture and its composition indicates ranging between granitic to dioritic in composition. The geochemical features of the granite indicate I-type and subalkaline nature of the granitic body.

The geochemical signatures of the Kavacık granite points out a volcanic arc setting as similarly seen in the Karaburun granite. U-Pb zircon LA ages were also obtained from the Kavacık granite ranging between 224.5 ± 2.0 My and 230.0 ± 2.8 My. Early Triassic zircon ages are also previously observed in the Karaburun Peninsula (Karaburun Granite) and the Menderes Massif (Ödemiş-Kiraz Submassif).

Keywords: Bornova melange, Early Triassic, I-type granite, U-Pb zircon ages, West Turkey, İzmir-Ankara Zone

BORNOVA KARMAŞIĞI'NDAKİ KAVACIK GRANİTİNİN YAPISAL VE DOKUSAL ÖZELLİKLERİ

ÖZ

Bornova karmaşığı, İzmir Ankara kenet kuşağı ile Menderes Masifi arasında KB-GB uzanan bir melanj temsil edilir. Bornova karmaşığı çoğunlukla ileri derecede deforme olmuş Geç Kretase-Geç Paleosen yaşlı kumtaşı ve şeyl karmaşığı, Mesozoyik yaşlı platform kireçtaşları ve okyanusal kabuk kayalarından oluşur. Bornova karmaşığı'nın matrisindeki bloklar çoğunlukla kireçtaşı, spilit, serpantinit ve radyolaryalı çörtler olarak tanımlanmaktadır. Bu çalışmada Bornova karmaşığı'nda yer alan, Kavacık tektonik dilimi olarak adlanan adlandırılan granitik kayaçların jeokronolojisi zirkon kristalleşme yaşları U-Pb izotoplarıyla ilk kez incelenmiştir. Kavacık tektonik dilimini oluşturan granitoitik kayalar tipik bir holokristalin doku gösterir. Granitoidlerin jeokimyasal özellikleri I-tipi ve subalkalin karakterli olduklarını ve oluşum ortamı olarak da bir volkanik yay ortamını işaret etmektedir. Kavacık tektonik diliminin birincil dokanak ilişkisi sahada net değildir ve Bornova karmaşığı içinde tektonik dilim halinde bulunmaktadır. Kavacık tektonik diliminde bulunan lökogranitilerden ayrılan zirkonların U-Pb izotoplarının lazer ablation yöntemiyle elde edilen yaşları 224,5 ± 2,0 My ve 230,0 ± 2,8 My arasında değişmektedir.

Daha önce Karaburun Yarımadası'nda (Karaburun Graniti) ve Menderes Masifi'nde (Ödemiş-Kiraz Submasifi) Erken Triyas zirkon yaşları gözlenmiştir, ancak Kavacık tektonik diliminde bulunan granititoidlerin dokusal ve jeokimyasal karakteri diğerlerinden farklıdır.

Anahtar kelimeler: Bornova melanjı, Erken Triyas, I-tipi granit, U-Pb zirkon yaşlandırması, Batı Türkiye, İzmir-Ankara Zonu

CONTENTS

LIST OF FIGURES

LIST OF TABLES

Page

CHAPTER ONE
INTRODUCTION

1.1 Location and Accessibility

In west Turkey, the Bornova melange as a part of the İzmir-Ankara Zone, forms one of the main tectonic belts of the Aegean Region (Figure 1.1). The NE-trending Bornova melange is located between the Menderes Massif and the Sakarya Zone of the Pontides. The thickhest part of the Bornova melange crops out around İzmir, and the study area is situated between Seferihisar and İzmir, and 30 kilometers to the southwest of İzmir City Center.

The study area includes some parts of the 1/25000 scale topographic maps of İzmir L17b3 and L18a4 sheets and it covers an area of approximately 40 square kilometers. The sudy area is located in the northwest of the Kavacık Village and the altitude ranges from 700 meters to 1000 meters (Figure 1.1 and Plate I).

In the area between Seferihisar and İzmir, the Bornova melange is represented by huge blocks of platform limestones and strongly sheared sandstone-mudstone matrix with thin intercalations of calcereous shales. In addition to these blocks of platform limestones the Bornova melange contains tectonic slices composed of serpentinites and mafic volcanics (spilites). The melange formed during closure of the Neotethys between the Sakarya Zone and the Anatolides were named as the Bornova melange by Erdoğan (1990 a, b) and the Bornova Flysh Zone by Okay & Altıner (2007). In this thesis, from the view point of nomenclature the Bornova melange is followed.

1.2 Objectives

In west Turkey, from east to west, Menderes Massif, Bornova melange with the Karaburun belt and the Sakarya Zone form the main tectonic belts (Figure 1.1). The Bornova melange exteds between İzmir and Balıkesir, an is represented by a regional olistostrome/melange belt between Sakarya Zone and Menderes Massif. Erdoğan

(1990) described huge limestone blocks in the in Late Cretaceous-Danian flysch matrix and tectonic slices of ophiolitic rocks in the Bornova melange.

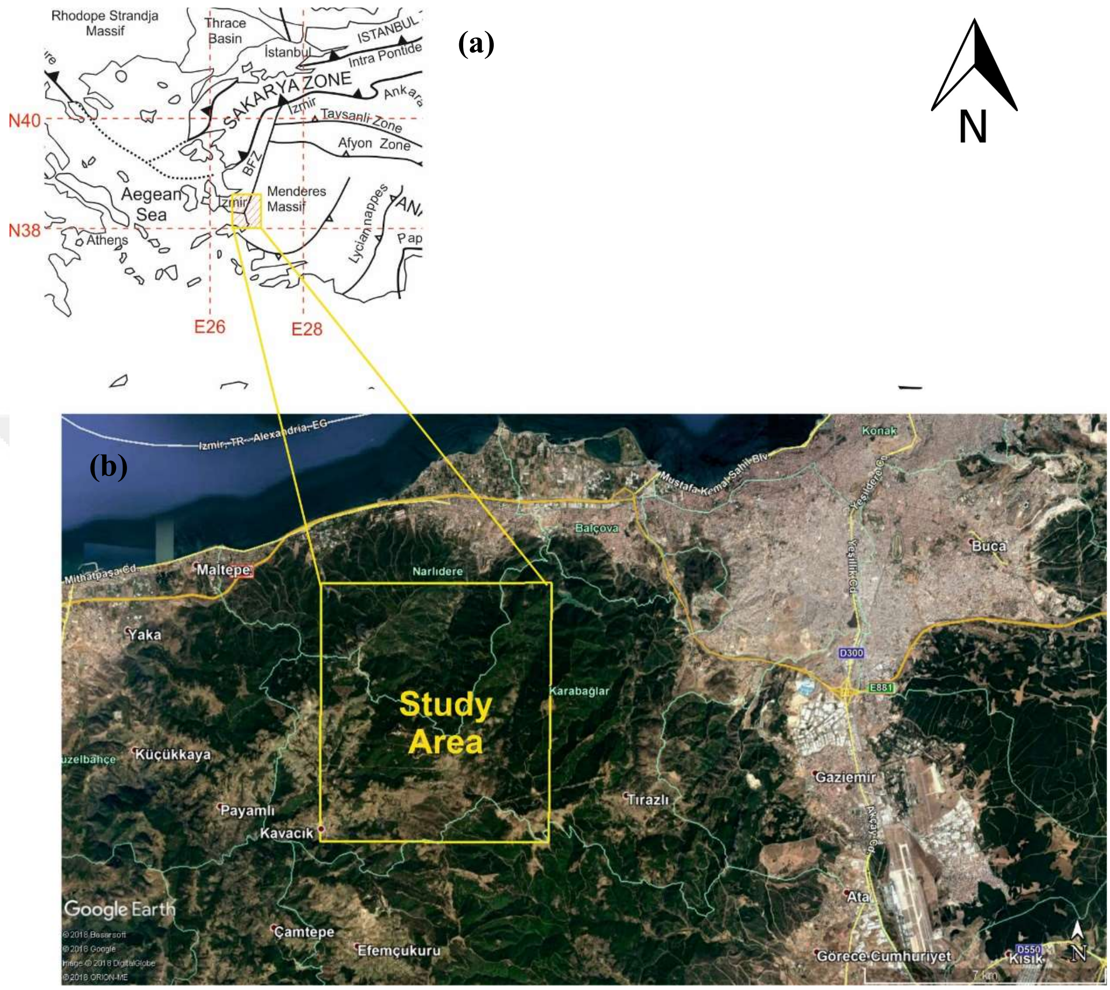

Figure 1.1 Map showing the main tectonic belts of western Turkey (Okay & Tüysüz, 1999) and location of the study area (Google Earth, 2016)

Although the flysch-type sediments and ophiolitic rocks of the Bornova melange were studied in detail, there is no study about granitic rocks that incorporated into the Bornova melange in the Kavacık area. This granitic rocks were described by Öngür (1972) in unpublished report (MTA) focused on the geothermal features of the area extending between İzmir and Urla. To disclose the tectonic position, petrography, geochemistry and geochronology of these granitic rocks are the aims of this study.

1.2.1 Scope and Methods of Study

The main aim of this thesis is to map the granitic rocks that crop out around Kavacık Village in the Bornova Melange. *Geological mapping* was carried out in 1/25000 scale around Kavacık Village. During the field work the contact relations and extend of the granitic rocks in the Bornova Melange were observed along cross-sections. Along these cross-sections structural measurements were made and, systematic and oriented samples were taken. *Petrographic analysis* was carrid out in the field by naked-eye and lup in the field, and then by thin section analysis in microscopic studies. *Geochemical analysis* includes major oxides, trace elements, rare earth elements (REE) values were obtained by geochemical analyses done in the ACME (Canada). These results were used to determine the nomenclature, character and tectonic setting of the granitic rocks in the study area. Zircons for the geochronologic analysis (U/Pb) were were seperated from the granitic rocks in the study area. The seperated zircons were used in the radiogenic measurement in the Mainz University (Germany). *Structural analysis* was performed along the cross-section lines in the field by measuring the planar and linear structures in the outcrops oriented perpendicular the foliation and parallel to the lineations. In addition to this observatios, oriented thin sections were examined for the kinematic analysis. The structural data measured were interpreted by the contour diagrams. Geological mapping, geochemical analysis and geochronological features of the granitic rocks help us to interpret the relations to the Efemçukuru gold deposit and Balçova geothermal field. Besides, these analysis provide new data that reveal evolution of İzmir-Ankara Zone, one of the main tectonic belts of west Turkey, and therefore closure of the Neotethys.

1.3 Guideline of Thesis

This thesis is prepared according to the postgraduate thesis writing rules realesed by the Graduate School of Natural and Applied Sciences in Dokuz Eylül University, İzmir. This thesis consists of six parts. First chapter introduces the location of the study area, the purpose of the study, methods used, and previous studies in the study area and surrounding. The second chapter includes lithologic description of the tectonic slices of Bornova melange in the Kavacık area. Nomenclature, geochemistry, petrography and tectonic setting of the granitic rocks in the study area are presented in the third chapter. In the fourth chapter, radiogenic dating of the granitic rocks is revealed. The structural features and kinematics of the tectonic slices in the study area are described in the fifth chapter. Results of this study and discussion will be presented in the last chapter. The details of methods for mineral separating, radiogenic dating, geochemical analysis and structural measurements are given as appendix. Geological map and crass-sections of the study area are given as separate plate at the end of the thesis.

1.4 Previous studies

In the Kavacık area, there are few researches reported previously and the ones subjecting the study area are listed below.

Akartuna (1962) divided the Menderes Massif into mica schists and marbles located in the region and pointed out that the contacts between the flysch-type rocks of İzmir-Ankara Zone and the neritic limestones are problematic.

Brinkman (1966, 1972, 1976) reported that the İzmir-Ankara Zone is composed of sandstones and shales with radiolarian cherts and ophiolitic rocks.

Konuk (1977) was mapped the base of the Bornova Flysch. The paleontologic data presented in this previous study show that the age of the Bornova Flysch is the Late Maastrichtian-Palaeocene the around Bornova.

In the Gümüldür region, the lower contact of the Bornova melange with the Menderes Massif was described as an approximately flat thrust fault along which the Bornova melange emplaced on the crystalline rocks of the Menderes Massif during the Late Eocene-Oligocene interval (Başarır & Konuk, 1981). The Bornova melange is represented by huge blocks of Triassic-Liassic dolomites and limestones and the Late Cretaceous sandstone-shale matrix with mictiric limestones lenses that contain planctic foraminifers. The Menderes Massif is composed of micaschists and marbles showing a greenschist-facies metamorphism.

Özer & İrtem (1982) described platform limestones of Late Turonian-Late Maastrichtian age in the Bornova melange in the Işıklar-Altındağ region. The contact between the platform limestones and the sandtone shale alternation with Danian calcereous shales is fault.

The close resemblances between the neritic limestones block in the Bornova melange around Kemalpaşa and the western Taurus limestone platform were revealed by Poisson & Şahinci (1988).

Sarı (2013) focused on the calcareous shales outcrops located in Kocaçay, Pınarbaşı and Gökdere subareas in the Bornova melange. The planctic foraminifera assembledge in the these calcereous shales indicates an age range from the Late Maastrichtian to the Thanetian. This new age desciription revises the maximum deposition age of the matrix of the Bornova melange as the Thanetian.

Erdoğan (1990a) described the resemblances between the Karaburun carbonate platform sequence and huge limestone blocks between Bornova and Manisa. Erdoğan (1993b) introduced the stratigraphic and tectonic relations between the Karaburun belt and the Bornova melange: it is revealed that the Karaburun belt is a huge block in the Bornova melange. The similar blocks of Karaburun belt are found in the area between Manisa and Bornova.

Oyman (2003) revealed that there is a Miocene epithermal gold deposit in the Bornova melange in the Efemçukuru area, to the south of the Kavacık Village.

Bornova melange forms a tectonic zone with 50 to 90 km in width and approximately 230 km long to the northwest of the Menderes Massif along the İzmir-Ankara suture belt (Okay & Altiner, 2007). Besides limestone blocks of different sizes in the Bornova melange, the other blocks are composed of basalts, serpentinites and cherts.

Okay et al. (2012) suggested that the Bornova melange was formed in a narrow basin adjacent to a strike-slip fault zone due to the ophiolite emplacement from the northern part of the Anatolid-Tauride block during the closure of the Neotethys during the Late Cretaceous. The blocks of the Bornova melange are the Mesozoic limestones, sheared sandstones and shales and ophiolitic rocks. The limestone blocks form the majority of they are of two types: (i) Late Triassic-Cretaceous platform carbonates and (ii) Late Triassic pelagic limestones.

Models for the formation of the Bornova melange as follows: (i) an accretionary prism in the subduction zone (Erdoğan, 1990 a, b) and (ii) a blocky flysch zone in a basin adjacent to a strike-slip fault zone (Okay et al. 2012).

CHAPTER TWO
TECTONIC SLICES OF THE BORNOVA MELANGE IN THE KAVACIK AREA

Karaburun belt, Menderes Massif, Sakarya zone and İzmir-Ankara Zone are the main tectonic belts of the west Turkey (Figure 2.1). The Menderes Massif is made up of the nappes showing polymetamorphic events (Bozkurt and Oberhansli, 2001 and references therein). These tectonic slices were named as the Bayındır, Bozdağ, Çine and Selimiye nappes in the sturucturally ascending order (Ring at al., 1999; Gessner et al., 2001). This nappe pile was divided into northern, central and southern sub-massifs by low-angle normal faults in a rolling hinge model (Gessner et al., 2001). The Karaburun belt is made up of a Paleozoic detrital sequence, and Mesozoic platform carbonates. Regionally, the Bornova melange is represented by an ophiolitic complex around Akhisar and it is mainly characterised by flysch-type sediments around Bornova. The Bornova Melange in the west Turkey is a part of the İzmir - Ankara Zone. The matrix of Bornova Melange consists of fossil-free flysch-type sediments (Sarı, 2013). Platform-type limestone blocks, spilites, chert and serpentinite blocks are located in matrix (Erdoğan,1990). The micritic limestones and red calcareous shales contain planktonic foraminifera indicating an age range between Maastrichtian and Thanethian (Sarı, 2013).

In the region between İzmir and Seferihisar, the Bornova melange is composed of tectonic slices of sandstone-shale, mafic volcanics (spilites), serpentinites, granites and huge limestone blocks in a sandstone-shale matrix with lenses of calcereous shales. In the study area (Plate I) to the northeast Kavacık Village, the Bornova melange is divided into four tectonic slices in the structurally ascending order as follows:

- Kayabaşı tectonic slice,
- Boytaş tectonic slice,
- Kavacık tectonic slice,
- Çatalkaya tectonic slice.

The common structural feature of these four tectonic slices is to be strongly sheared. This shearing forms a prominent foliation and linear fabric in all tectonic slices. All tectonic slices mainly strike NE and moderately dips to NW (Plate I).

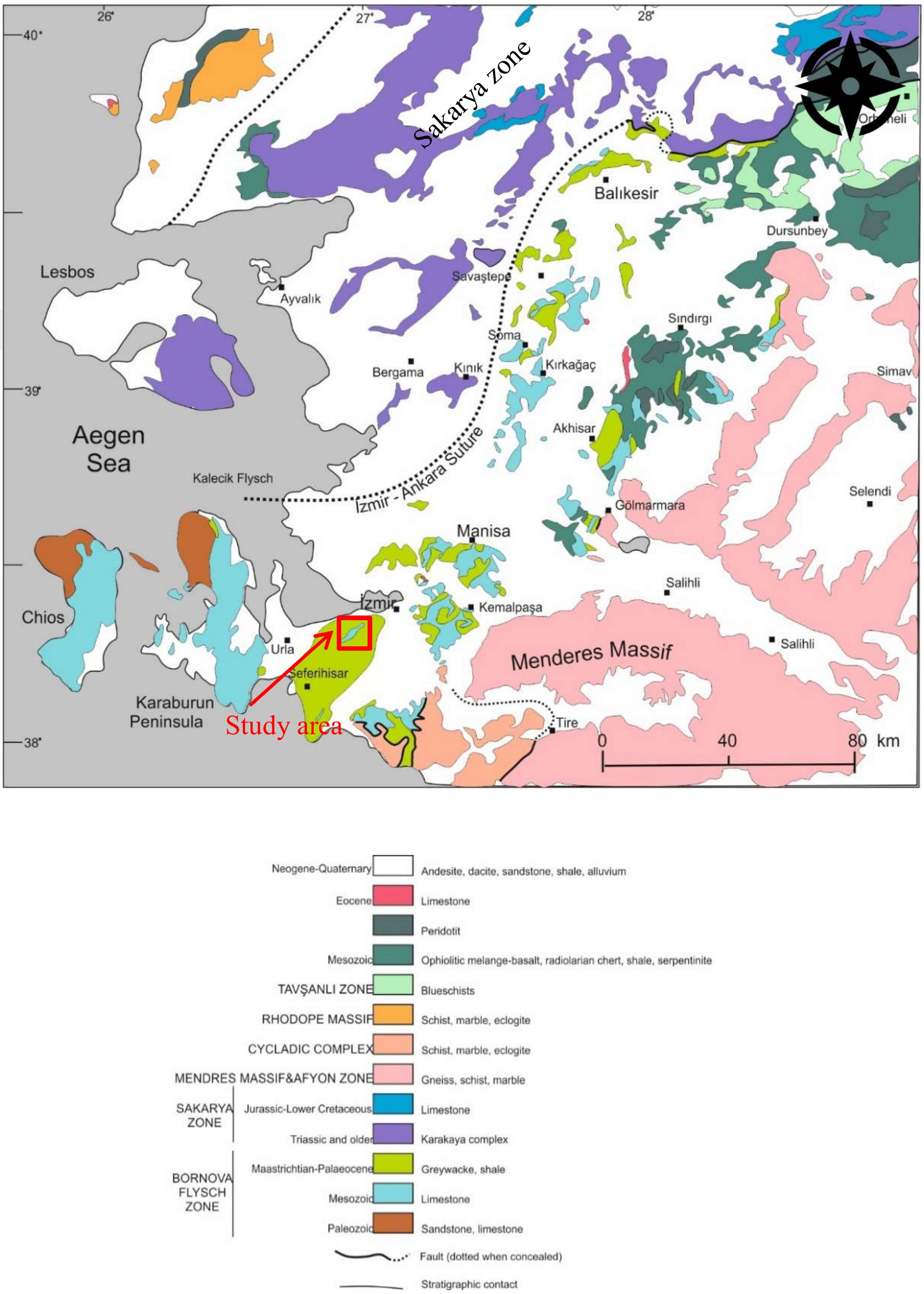

Figure 2.1 Simplified Geological Map of West Turkey (Okay et al., 2012)

2.1 Kayabaşı Tectonic Slice

The Kayabaşı tectonic slice is located in the east part of the study area (Plate I), and it occupies the structurally lowest position. This tectonic slice is made up of strongly sheared serpentinites, spilites, recrystallized limestones, radiolarian cherts, phyllites, low-grade metamorphic rocks (micaschists) and sandstone-shale alternation with thin limestone lenses. And it also contains undeformed rhyolite dykes that yields a 12 Ma U-Pb age.

Serpentinites in the Kayabaşı Tectonic Slice show a prominent foliation parallel to the elongation of the tectonic slice (Figure 2.3). Foliation in the serpentinites strikes northeast and dip moderately to northwest.

Figure 2.3 Foliated serpentinites in the Kayabaşı Tectonic Slice. Foliation strikes NE and dip to NW. Yellow line is parallel to the foliation [0498840; 4241643] 817 m. (Personal archive, 2016)

In the Kayabaşı Tectonic Slice, there are thin slices of strongly sheared sandstones and mudstones (Figure 2.4.a). In some parts of this highly sheared tectonic slice the primary stratification can be diagnosed by thin limestone lenses (Figure 2.4.c).

The sandstones both in the Kayabaşı and Çatalkaya tectonic slices show rough foliation diagnosed by thin cleavage domains. These domains are represented by disconnected, small and dark seamletts around sand grains (Figure 2.5.a, b). Besides this, in the pressure shadows around the large quartz and feldspar grains the mica beards composed of tiny sericites and fibrous quartz describes the rough foliation in sandstones.

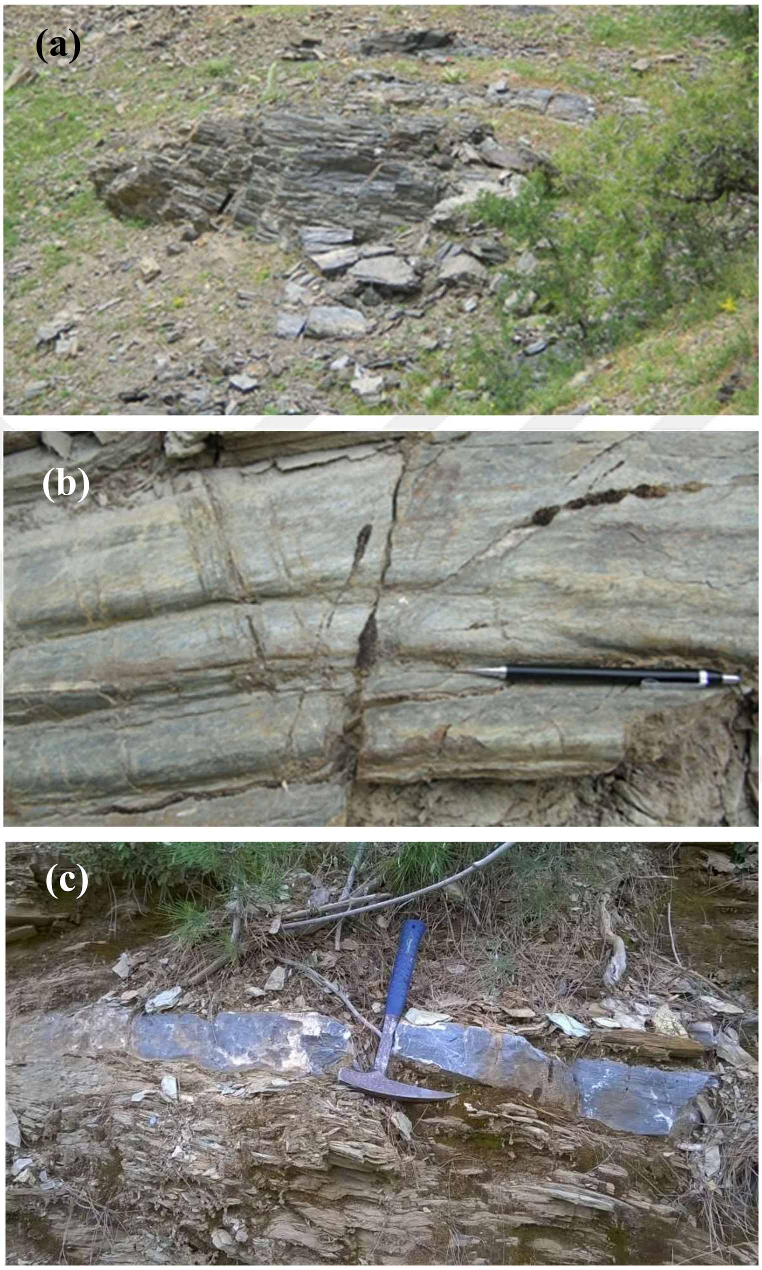

Figure 2.4 a) In the Kayabaşı Tectonic Slice, the sandstone-mudstone complex shows an anastomosing foliation. [0499840; 4242112] 811 m. b) Folded foliation in the phyllitic part of the Kayabaşı Tectonic Slice to the southeast of Kavacık Village. Pencil is parallel to the axis of mesoscopic folds. [0501172; 4244953] c) Thin limestone lenses in the sandstone-mudstone complex (Personal archive, 2016)

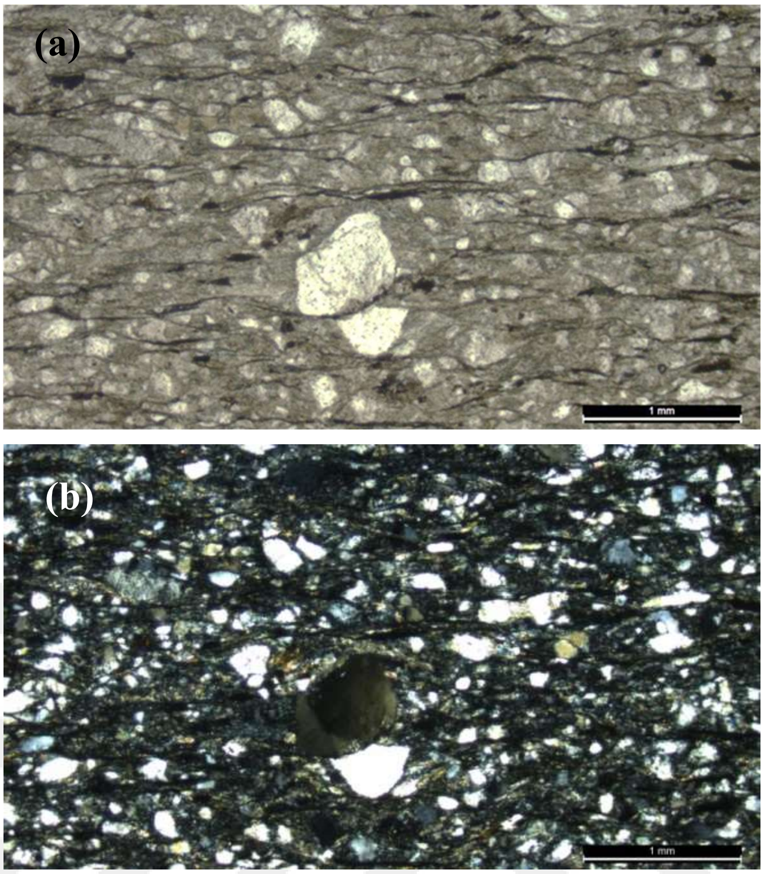

Figure 2.5 Photomicrography views of the sandstones with rough foliation along the upper contact of the Kavacık tectonic slice. a parallel light view (PPL), b cross light view (CPL)

Mafic volanics in the Kayabaşı Tectonic Slice is represented by green, spilitic basalt lava (Figure 2.6.a) and coarse-grained hyaloclatites (Figure 2.6.b,c). Close to the contact zones clasts and matrix represented by aquagene tuffs show an alignment (Figure 2.6.b,c). Long axis of the clasts and oriented matrix form the linear fabric in this tectonic slice.

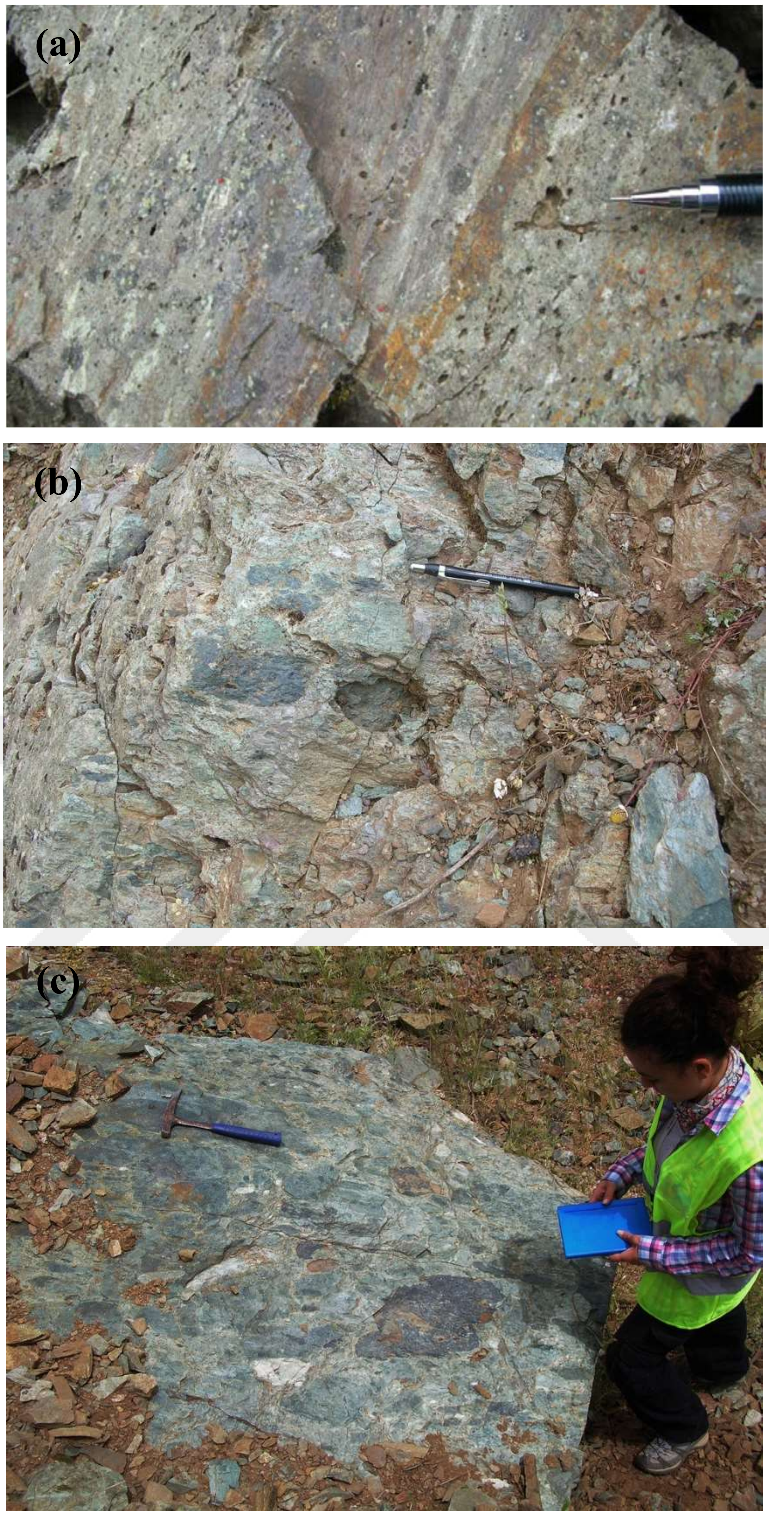

Figure 2.6 a) Close view of mafic hyaloclastics in the Kayabaşı Tectonic Slice. b) Coarse grained hyaloclastics. Preferred orientation of the clasts indicates a prominent deformation during the tectonic piling of the Bornova melange. Pencil (14 cm) is parallel to the long axis of elongated hyaloclasts. [0496914; 4227993] 284 m. (Personal archive, 2016)

Gray micaschists in the Kayabaşı Tectonic Slice are composed of quartz and muscovite (Figure 2.7.a). Long axis of quartz grains and muscovites define a continuous foliation. Quartz crystals between foliation planes defined by muscovite elongated parallel to the cleavage domains (Figure 2.7.b). Quartz crystal clearly show undulatory extinction and they are seriate and interlobated in form.

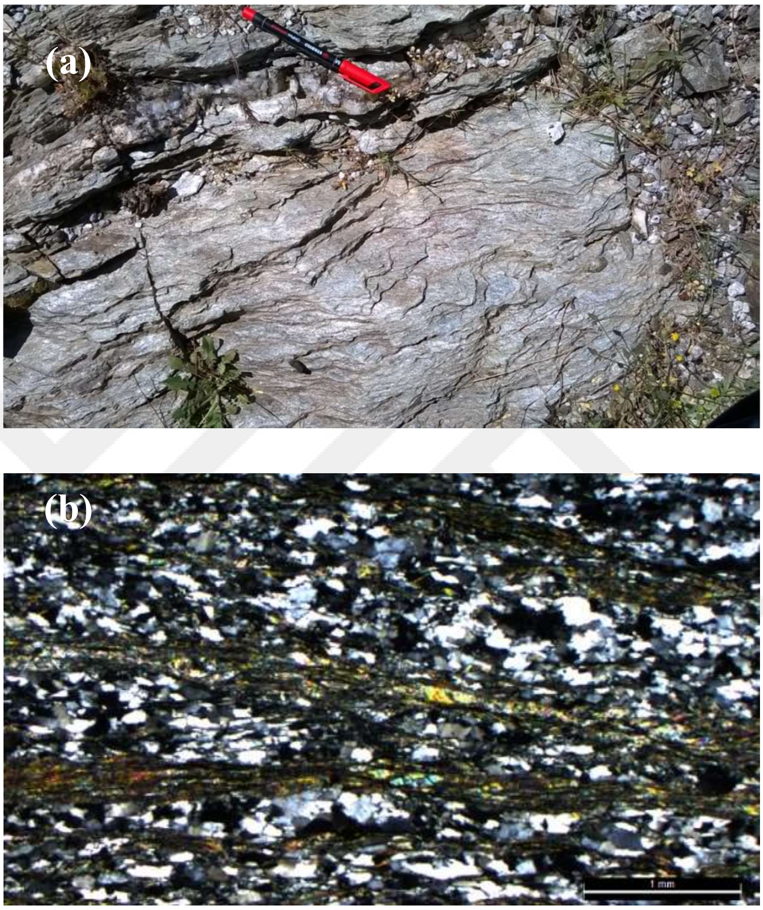

Figure 2.7 a) Micaschists are found as thin tectonic slice in the lower part of the Kayabaşı Tectonic Slice. These micaschists cut by undeformed dykes of rhyolites that yield 12 Ma U-Pb age. b) Microphotograph showing fine grained lepidoblastic tecture in gray micaschists [0500135; 4242842] (Personal archive, 2016)

Recrystallized limestones are found along upper contact of the Kayabaşı Tectonic Slice. They are represented by very fine-grained gray calcite crystals and show a continuous foliation and a prominent stretching lineation (Figure 2.8).

Figure 2.8 Field view of gray recrystallized limestones located at the structurally uppermost part of the Kayabaşı Tcetonic Slice. These limestones are strongly sheared. Along the foliation planes the stretching lineation is clearly observed [0500193; 4242956] (Personal archive, 2016)

The Kayabaşı Tectonic slice is structurally overlain by the Boytaş and Kavacık Tectonic Slices (Plate I), (Figure 2.9).

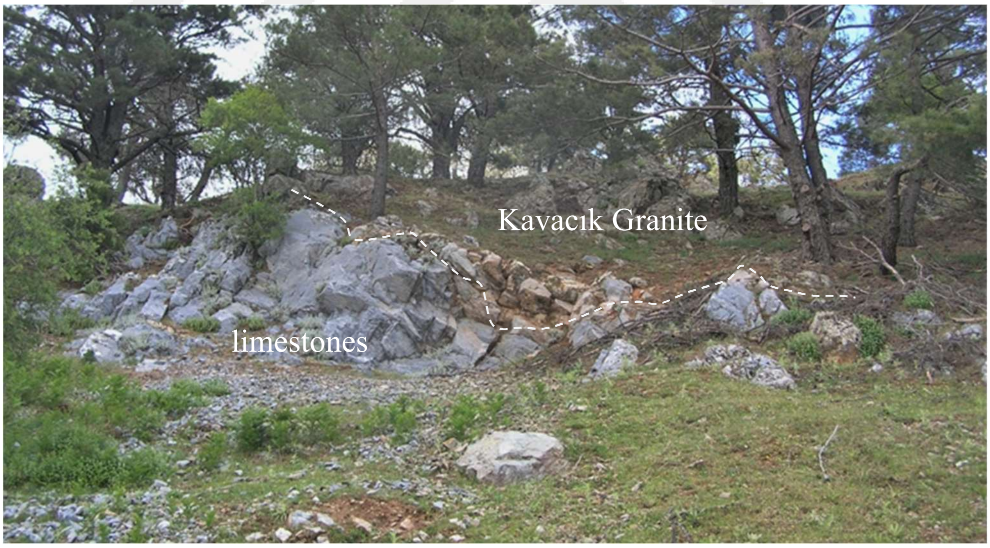

Figure 2.9 Contact between the Kayabaşı Tectonic Slice and the Kavacık Tectonic Slice (white dashed line). The lower part of the photograph is recrystallized limestones showing foliation and lineation. The upper part is the granites in the Kavacık Tectonic Slice. The yellow zone observed along the contact is represented by mylonitic granites [0500193; 4242956] (Personal archive, 2016)

2.2 Boytaş Tectonic Slice

Boytaş Tectonic Slice contains quartz sandstones, quartz conglomerates (Figure 2.10) and riyolite intercalations in mudstones (Figure 2.11). This tectonic slice is mapped as a discontinuous tectonic slice between the Kayabaşı and Kavacık Tectonic Slices (Plate I).

Figure 2.10 Quartz Conglomerates exposed to the northeast of Kavacık Village. The Boytaş Tectonic Slice showing an anastomosing foliation is sandwiched between the Kayabaşı and Kavacık Tectonic slices [0497488; 4241327] (Personal archive, 2016)

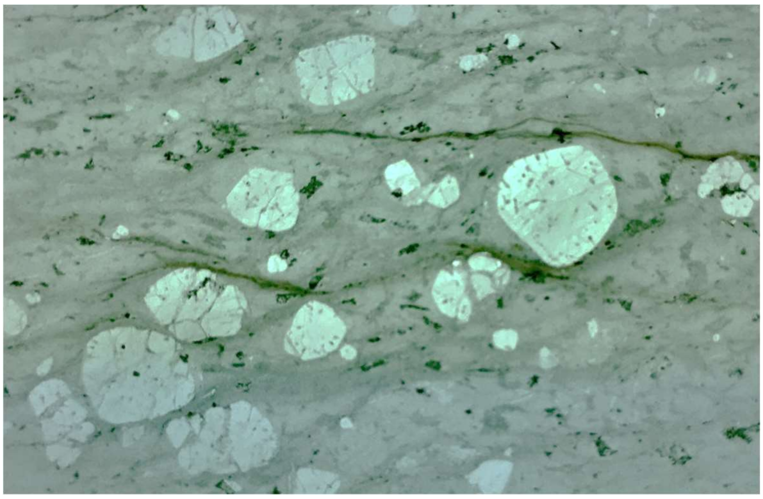

Figure 2.11 Photograph showing porphyritic texture of green rhyolites in the Boytaş Tectonic Slice. Large feldspar phenocristal of feldspar float in glassy matrix. Dark green cleavage domains indicate rough foliation. Width of view is 5 cm. (Personal archive, 2016)

2.3 Kavacık Tectonic Slices

The Kavacık Tectonic Slice is composed of plutonic and subvolcanic rocks that range in composition from gabbroic-diorites to granites (Figure 2.12).

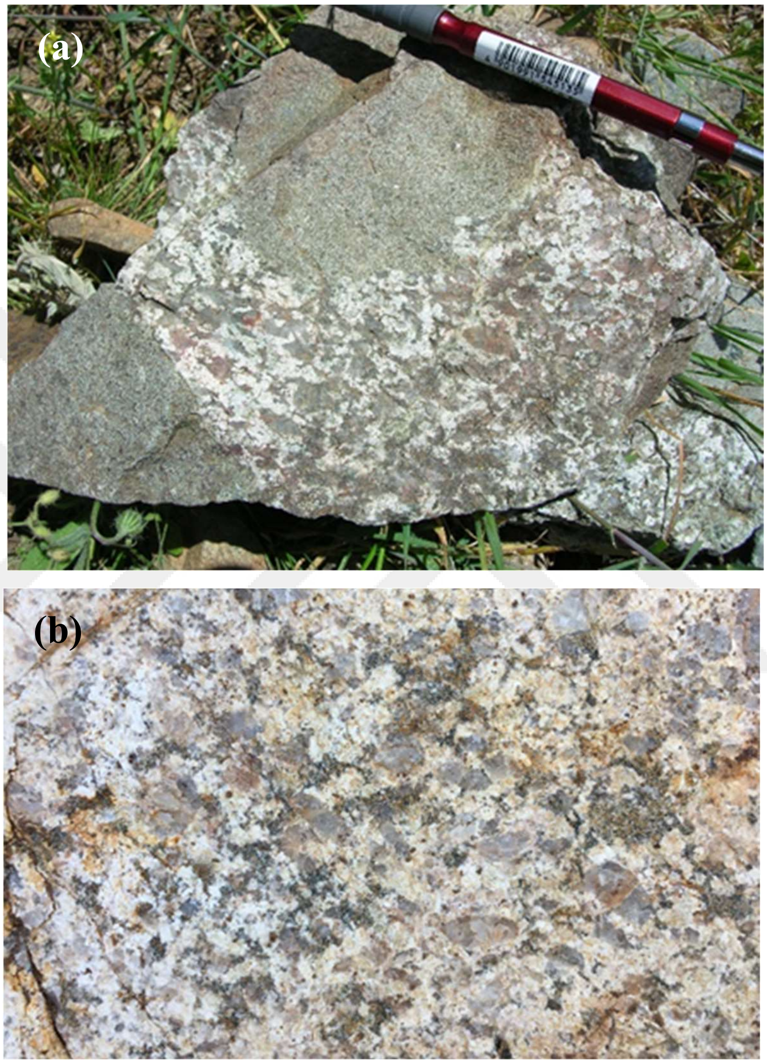

Figure 2.12 a. Coarse grained granite with fine grained mafic xenolits, size of block is 25 cm. Close view shows large quartz and feldspar crystals that make up the holocrystalline texture in the Kavacık Tectonic Slice, witdh of view is 10 cm. [0499561; 4242523] (Personal archive, 2016)

Geochemical characteristic of these magmatic rocks are described in detail in following chapter. The Kavacık Tectonic Slice is found on top of the Boytaş and Kayabaşı Tectonic Slices is composed of green diorites and leucocratic granites (Figure 2.13). Diorites and gabbroic diorites are dark green and finer grained than granites. Amphiboles, pyroxene and feldspar are the main minerals of diorites

(Figure 2.13.b). Leucocratic granites contain large size crystals of feldspar and quartz (Figure 2.12.a, b and Figure 2.13.a).

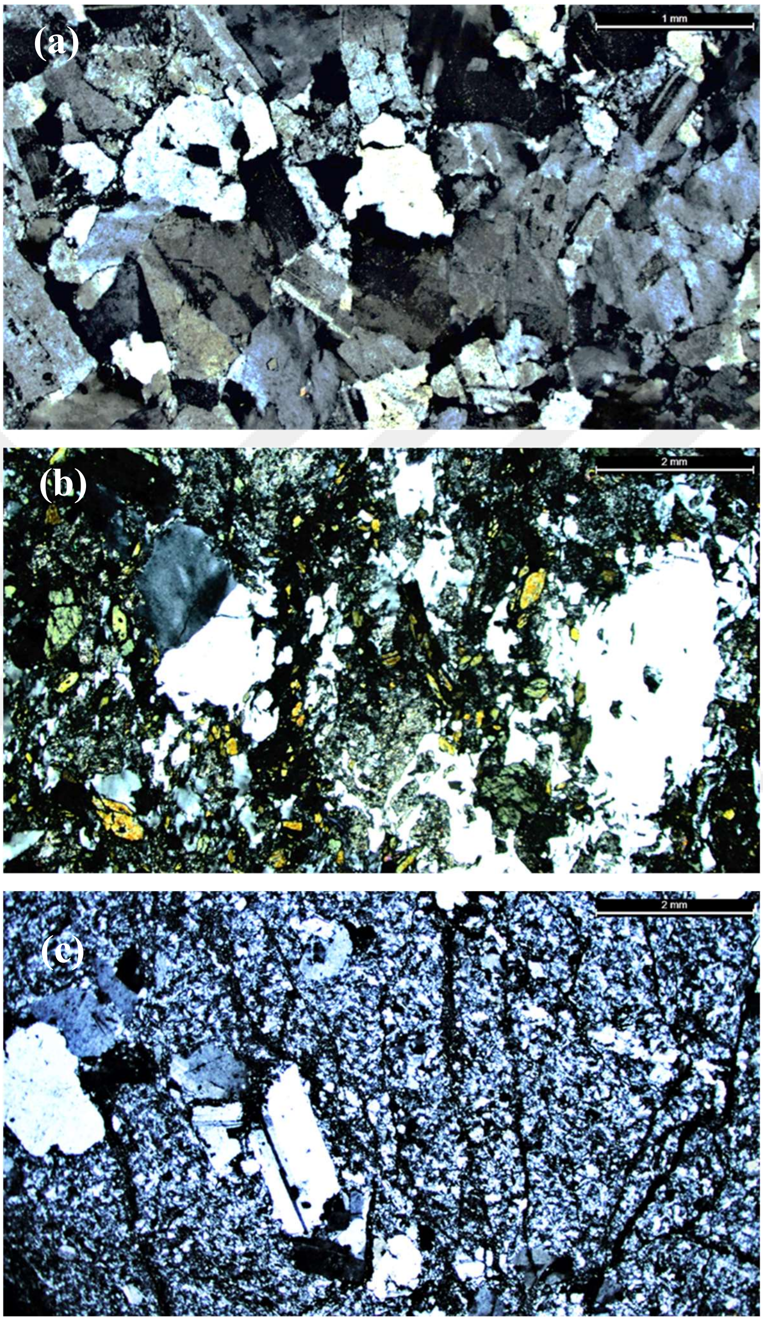

Figure 2.13 Primary textures (CPL) of igneous rocks in Kavacık Tectonic Slice. The top (a) microphotograph shows the holocrystalline texture of leucocratic granites. In the middle (b) is a microphotograph of diorite / gabbroic diorite of the holocrystalline texture. Below (c) is the view of (subvolcanic) granite porphyry (Personal archive, 2016)

The most of feldspar crystals show a strong saussuritization that defined by tiny serisite crystals and clay. These leucocratic granites clearly cut the finer grained mafic parts (Figure 2.12.a) while the leucocratic granites show a coarse-grained texture. The mafic component of the Kavacık Tectonic Slice show fine-grained holocrytalline texture (Figure 2.12.a).

Along the upper contact of the Kavacık Tectonic Slice the fine-grained, white color rocks show porphyric texture (Figure 2.13.c). Thin section studies of these rocks show that large feldspar and quartz crystals set in very fine garined matrix composed of quartz and feldspars.

In the Kavacık Tectonic Slice chloritization, epidotization and saussuritization types of alterations are observed. Chloritization is seen both in mafic and leucocratic parts in the Kavacık Tectonic Slice (Figure 2.14.a). While the chloritization is diffusive in granites and diorites, the epidotization is seen as small veins (Figure 2.14).

Figure 2.14 (a) Field view of epidotization and (b) field view of chloritization (Personal archive, 2016)

Epidotization is seen as small veins filled by acicular epidotes and quartz grew perpendicular the mode I crack (Figure 2.15.a). Chloritization is diagnosed by chlorite patches in thin section in and around of mafic minerals such as biotites and amphiboles (Figure 2.15.b). Both in the diorites and granites, the feldspars show intense saussuritization produced tiny serisite and quartz crytals as well as clay minerals (Figure 2.15.c).

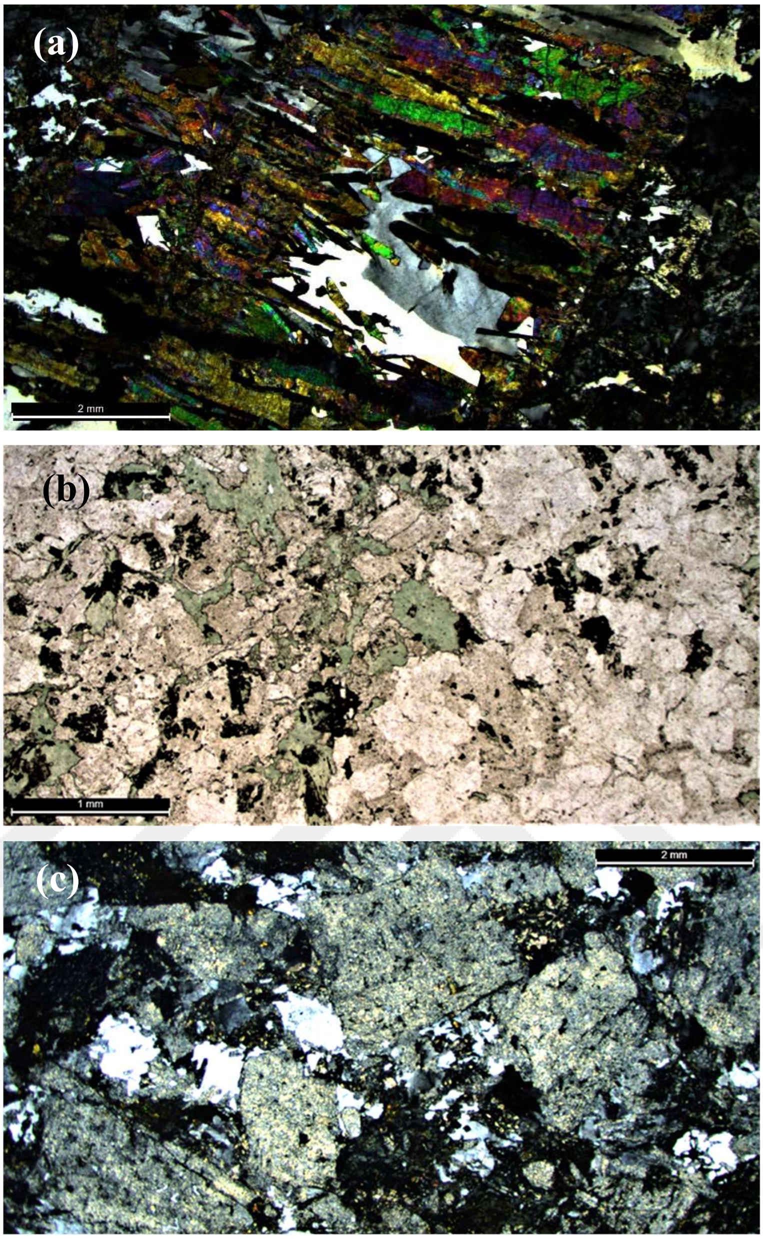

Figure 2.15 Microphotographs showing alteration types in Kavacık Granite: (a) epidotization, epidote and quartz fibers in mode I crack, CPL, (b) chloritization, chlorite patches indicate that mafic minerals altered into chlorite, PPL and (c) sosuritization, serisite (yellow parts) and tiny quartz in feldspars, CPL (Personal archive, 2017)

Along the contact zone of the Kavacık Tectnic Slice a strong deformation is recognized. All lithologies show both ductile and brittle deformation. Specially subvolcanic rocks show a prominent continuous foliation (Figure 2.16) and linear fabric along the foliation planes.

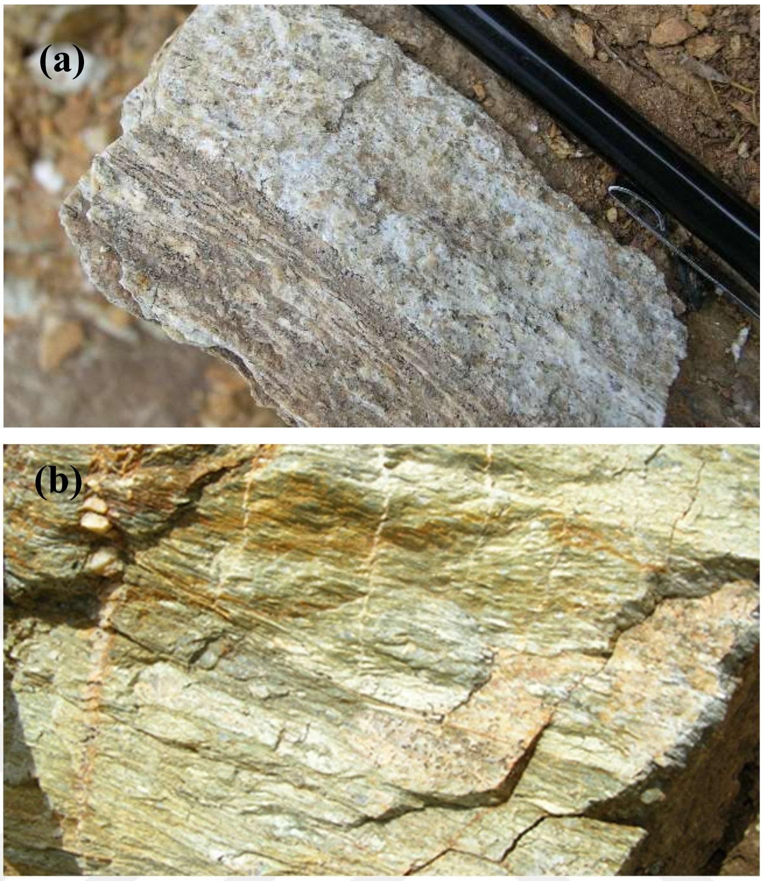

Figure 2.16 Close views of the mylonitic fabrics observed in Kavacık granite. A prominent mylonitic fabric observed along the contacts of the Kavacık Tectonic Slice [0500446; 4243432] (Personal archive, 2016)

Petrographic studies show that leucocratic granites also show cataclastic texture (Figure 2.17) diagnosed by disintegrated quartz and feldspar crystals. These broken crystals of feldspar and quartz show no preferred orientation. In strongly sheared part of the leucocratic granites show continuous foliation diagnosed by oriented quartz and feldspar crystals (Figure 2.18). In addition, pressure fringes around pyrite crystals also show ductile deformation in leucocratic granites.

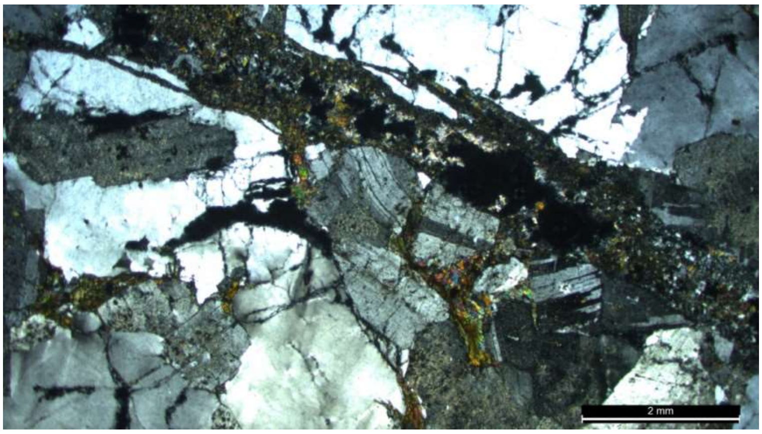

Figure 2.17 A thin section view of brittly deformed feldspar crystals [0497875; 4244202] (Personal archive, 2017)

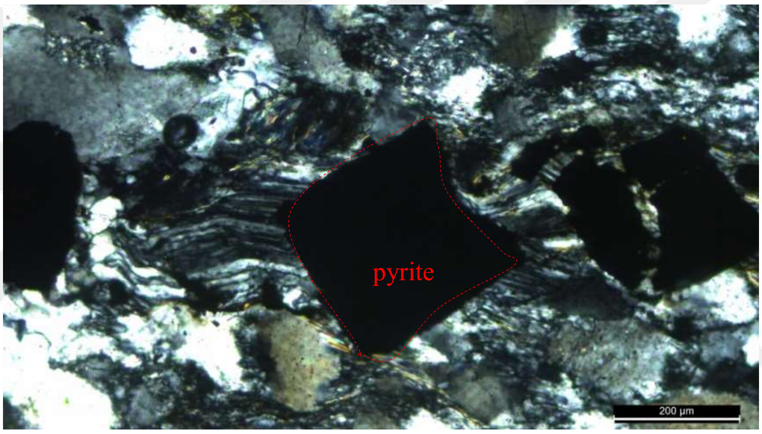

Figure 2.18 Pressure fringes white arrows around the pyrite crystal [0497875; 4244202] 751 m. (Personal archive, 2017)

Not only the granites in the Kavacık Tectonic Slice but also sandstones show a strong foliation in the Çatalkaya Tectonic Slice (Figure 2.19). Figure 2.19.a shows macroscopic features of foliation in sandstones. The foliation planes are closely spaced. Continuous cleavage planes can be seen in thin sections (Figure 2.19.b). Grain in microlithons are strongly oriented parallel to the cleavage planes. Around coarse grains, the mica beards composed of serisite and quartz are seen.

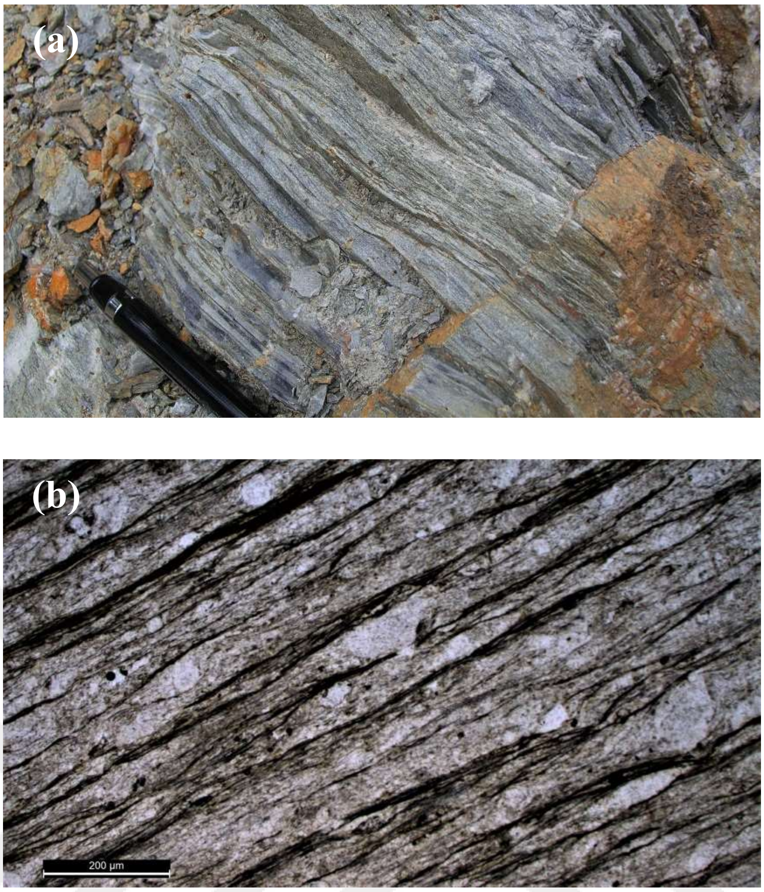

Figure 2.19 (a) Field view of foliated sandstones in Kavacık Tectonic Slice. (b) Microscopic view of these sandstones. Dark seams are cleavage domain and grains in microlithons were oriented parallel to these cleavage domains [0498039; 4244066] 650 m. (Personal archive, 2016)

2.4 Çatalkaya Tectonic Slice

The Çatalkaya Tectonic Slice is found on the Kavacık Tectonic Slice (Plate I) and is represented by sand stone-shale complex and limestone blocks along the hill top of NE trending Çatalkaya Mountain.

Sandstone-shale complex show anastomosing foliation the rootless folds are common (Figure 2.20.a). The axis of these folds mainly trend northeast and shallowly plunge to either northeast or southwest. To the northeast of the study area, the Çatalkaya Tectonic Slice comprise a sequence represented by proximal turbidites (Figure 2.20.b).

The parts of these turbidites contain conglomerates and fine conglomerates and show rough foliation indicated by preferred orientation of coarse grains and matrix.

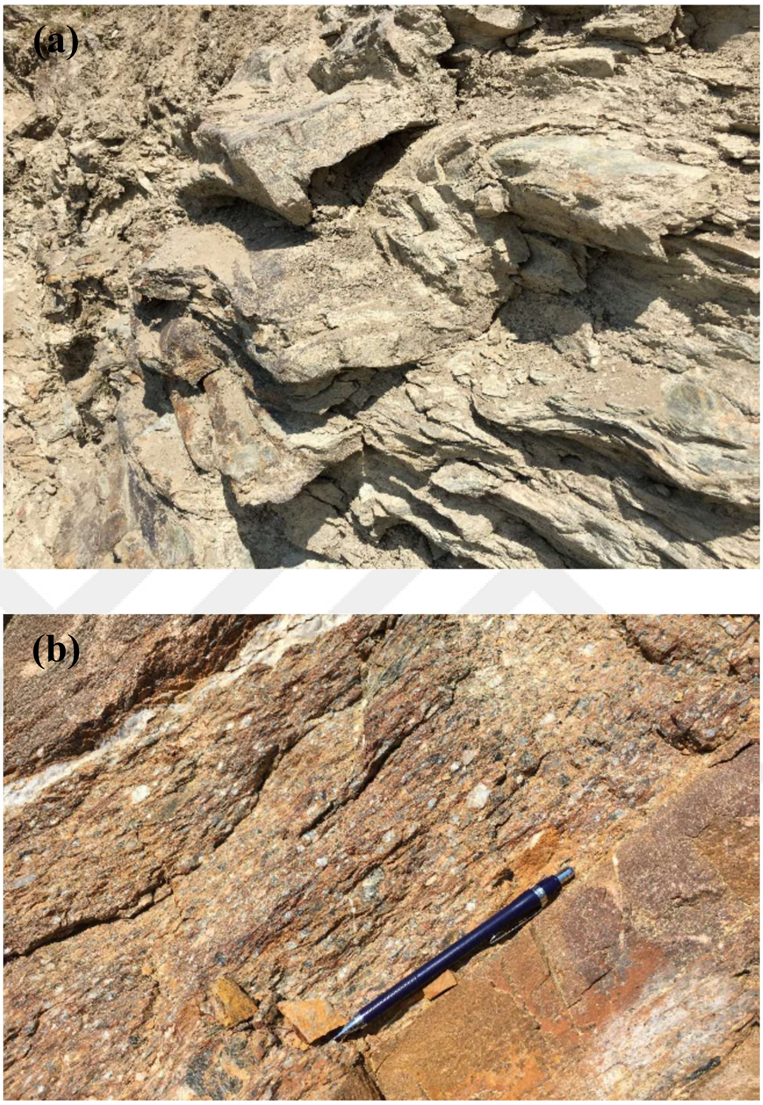

Figure 2.20 (a) Tight folds in the Çatalkaya Tectonic Slice. These folds are rootles and their axis trend to NE (b) Proximal turbidites diagnosed by conglomerates in Ta parts in the Çatalkaya Tectonic Slice (Personal archive, 2016)

CHAPTER THREE
GEOCHEMISTRY

Nomenclature, geochemical characteristics and tectonic setting of the magmatic rocks in Kavacık Tectonic Slice are examined by geochemical analysis including measuring their major oxides, trace and rare earth elements. The methods of these measurements are given at the end of this thesis in appendix.

For the geochemical anaylsis, 20 samples were taken from the Kavacık Tectonic slice. Major oxides, trace elements composition and LREE of the samples from the Kavacık Tectonic Slice are given in Table 1, in which SiO_2 ratios varies from %54.8 to %74.3, Al_2O_3 from %12.2 to %17.25, Fe_2O_3 from %1.64 to % 10.7, CaO from %.2.12 to % 7.03, MgO from %0.25 to % 5.04, Na_2O from %2.7 to % 5.68, K_2O from %0.24 to % 1.94, TiO_2 from %0.09 to % 0.89, MnO from %0.03 to % 0.20, P_2O_5 from %0.02 to % 0.13, SrO from %0.01 to % 0.03, BaO from %0.01 to % 0.05, LOI from %1.07 to % 5.96, and Cr_2O_3 <0.01 major oxides. (Results of the analysis were given in Table 1 in appendix).

The results of the geochemical analyses are plotted on related binary and ternary diagrams showing nomenclature, tectonic setting and characters of the plutonic rocks from Kavacık Tectonic Slice.

In the nomenclature diagrams devised by Whinchester Floyd (1977) based on their silica, alkali contents, and ratio of Zr/Ti, the samples scatter in the fields from gabbro to granite (Figure 3.1).

In order to determine major oxides attributes of the plutonic rocks from the Kavacık Tectonic Slice, geochemical data of the samples are ploted on the total alkalis versus silica diagram of Irvine & Bragar (1971) (Figure 3.2). All samples from the plutonic rocks plot in the subalkaline field. The the ternary diagram arranged by Irvine & Bragar (1971) based on FeO^t, Na_2O+K_2O and MgO was used to subdivide whether they are in tholeiitic or calcalkaline characters. Except one sample, all other plot in the field of calcalkaline.

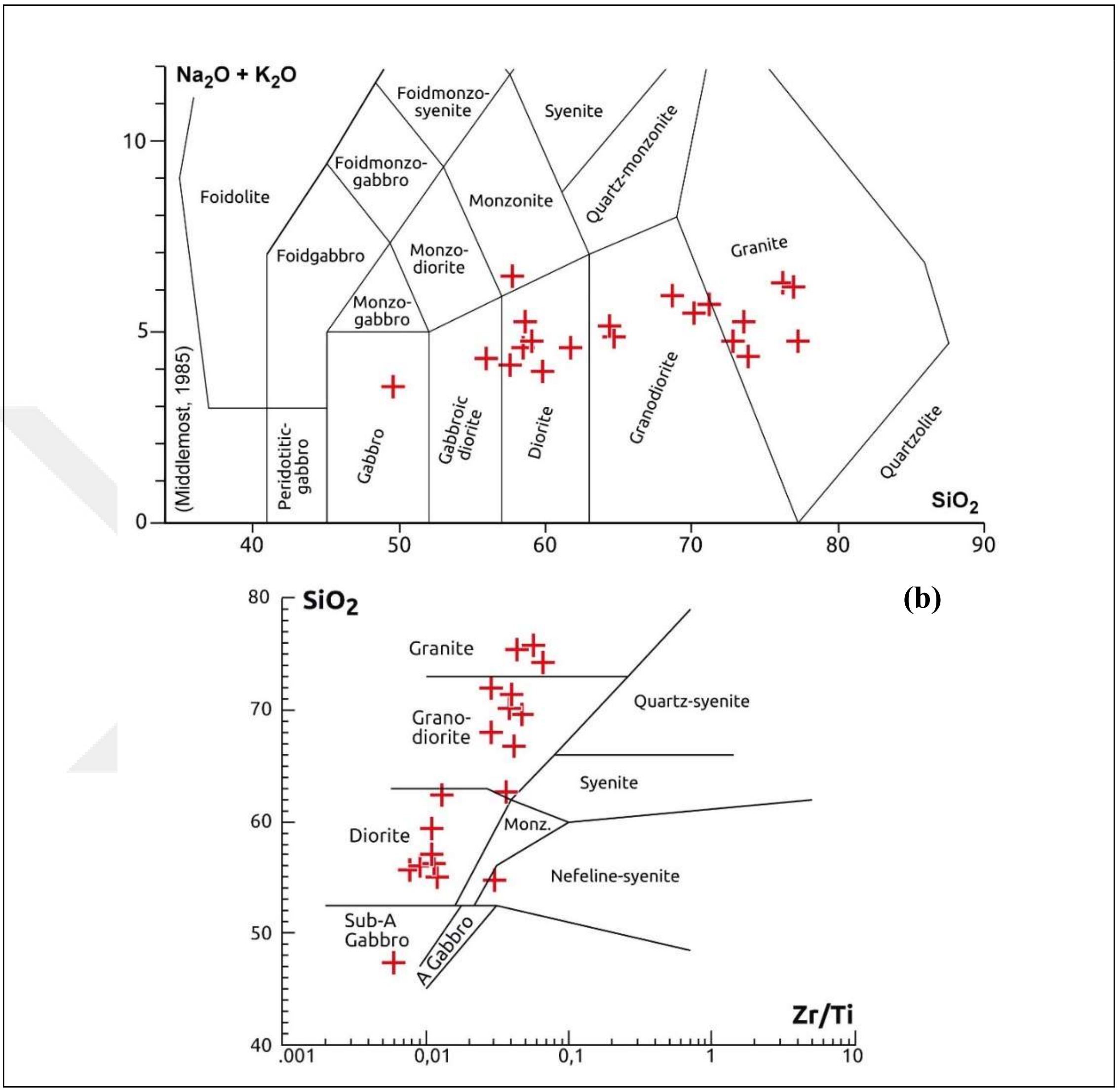

Figure 3.1 Nomenclature diagrams of the plutonic rocks from the Kavacık Tectonic Slice. In both diagrams, samples plot from gabbro to granite (a) Na_2O+K_2O - SiO_2 diagram (Middlemost, 1994) (b) SiO_2 – Zr/Ti (Winchester & Floyd, 19771)

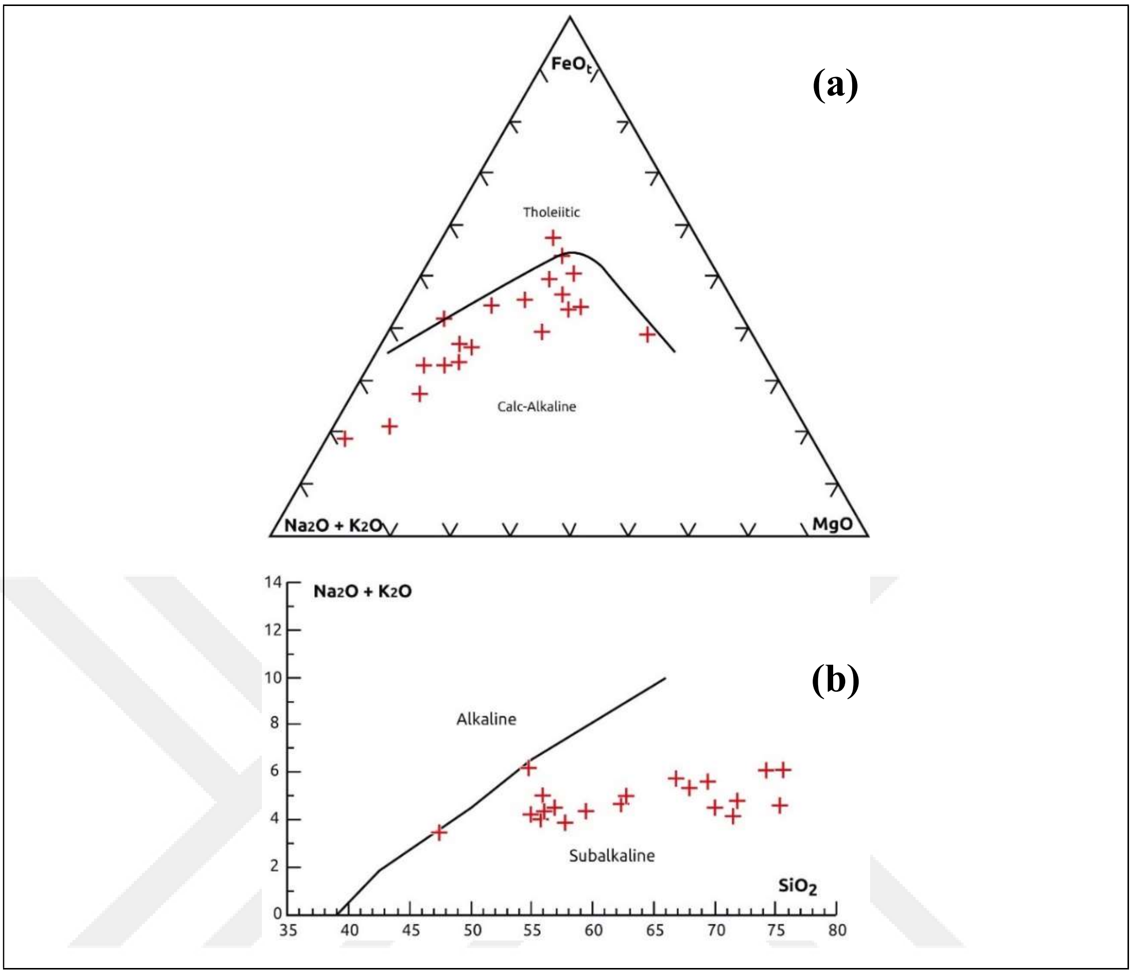

Figure 3.2 Diagrams showing the character of the magmatic rocks from the Kavacık Tektonic Slice (Irvine & Baragar, 1971). (a) Ternary diagram shows that the igneous in the Kavacık Tectonic Slice are calc-alkaline in character (b) Binary diagram shows that all samples set in the subalkaline field.

Geochemical characteristic of the plutonic rocks in the Kavacık Tectonic Slice are shown also on binary diagrams based on FeO^t / (FeO^t+MgO) vs. SiO_2, A/NK versus A/CNK and (Na_2O+K_2O)-CaO versus SiO_2 by Frost et al. (2001) (Figure 3.3). Figure 3.3.a show that a clear majority of the samples plot in the magnesian field, and Figure 3.3.b display that the most of samples plot in peraluminous field. These samples plot in calc-alkalic and calcic field separated equally (Figure 3.3.c).

The tectonic setting of the plutonic rocks from the Kavacık Tectonic Slice is examined by plotting their chemical data on related graphs combined by the elements that are considered to be relatively stable and insensitive to past emplacement alteration and effects of the metamorphism. The mobility of the elements have discussed in a number of studies, and the elements Rb, Hf, Ta, Y, Nb, Th are considered to be immobile during processes occurred post emplacement times.

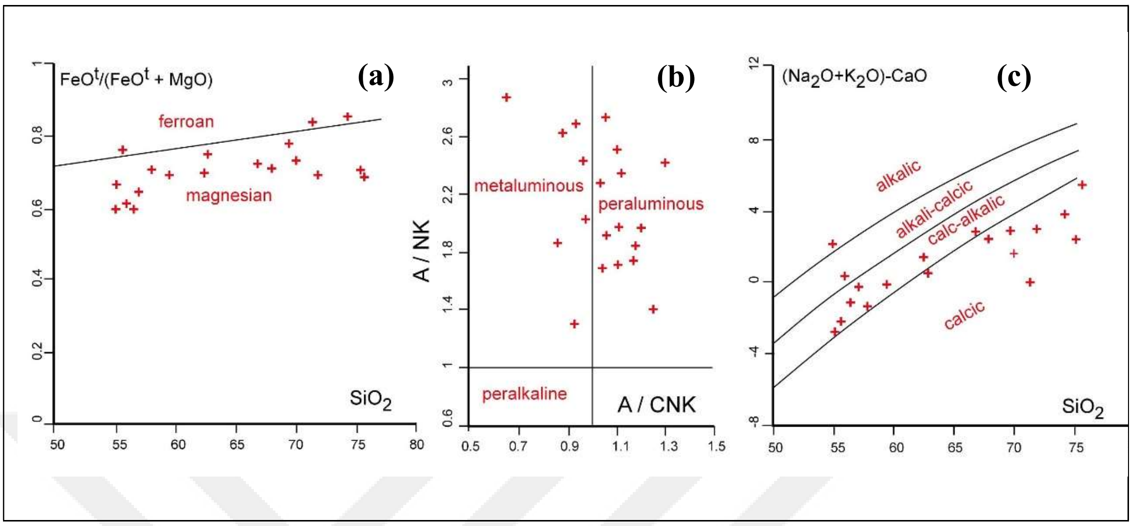

Figure 3.3 Diagrams showing igneous character of the plutonic rocks in the Kavacık Tectonic Slice (Frost et al., 2001)

The ternary diagram (Harris et al., 1986) in Figure 3.4.a clearly shot that almost all samples plot in the field of volcanic arc. The binary diagram combined by Th/Hf versus Ta/Hf displays that except one sample, the all samples plot in the field of active continental margin (Harris et al., 1986). The binary diagram (Pearce et al. 1984) clearly shows that samples from the Kavacık Tectonic Slice cluster in the field of volcanic arc granites. All of there three diagrams clearly shows that plutonic rocks in the Kavacık Tectonic Slice were formed in a continental volcanic arc.

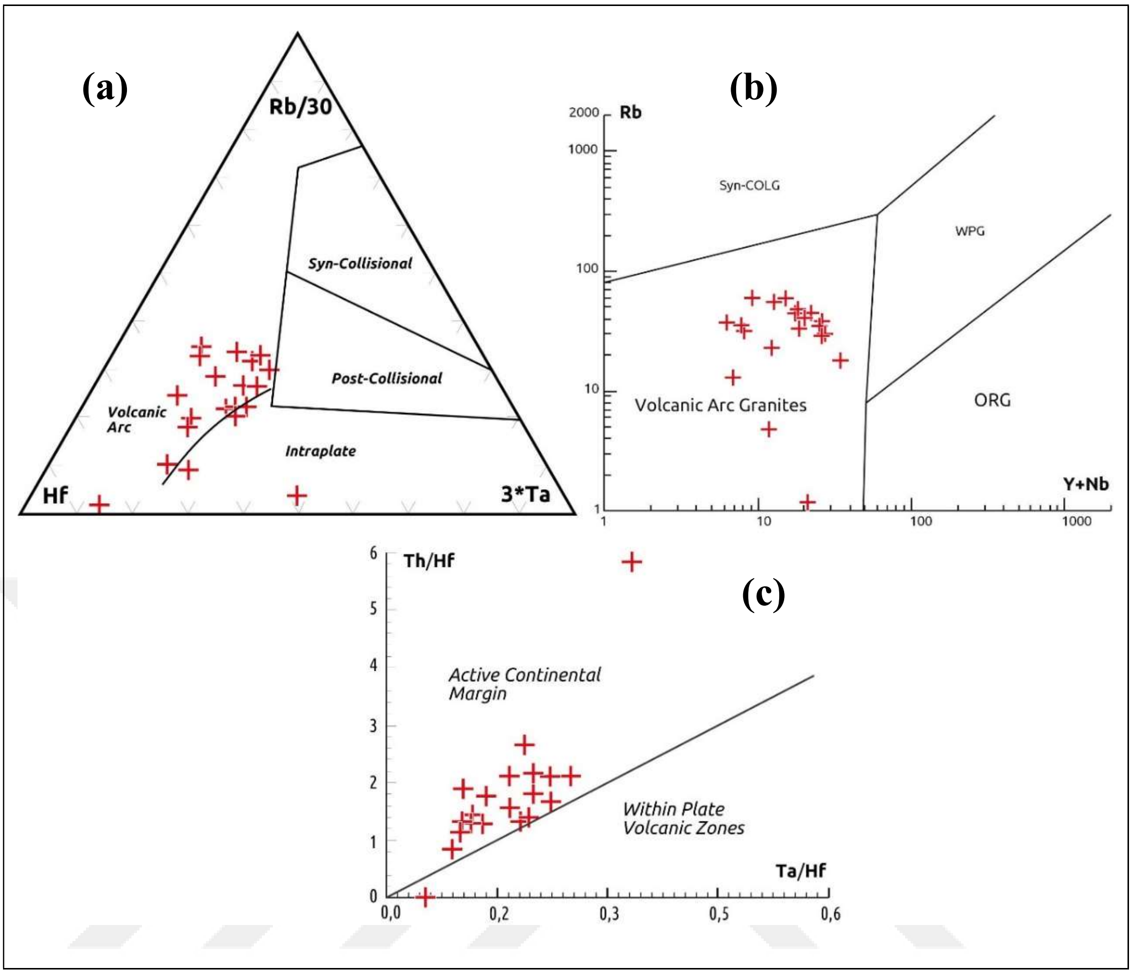

Figure 3.4 Geochemical diagrams show that Kavacık granite was formed in the magmatic arc environment (Harris et al., 1986; Pearce et al., 1984).

According to the rare earth patterns of plutonic rocks in the Kavacık Tectonic Slice felsic parts are enriched in comparision with the mafic parts. In both parts flat pattern in the LREE can be observed, however felsic parts (Leucocratic granites) are more enriched in LREE than the mafic parts (gabroicdiorites, diorites). Negative Eu anomaly is characteristic in leucocratic part, in where positive spike of Eu can be seen mafic part. Based on the felsic REE chemistry, volcanic arc granitoids chemistry features can be linked to the formation of the plutonic rocks in the Kavacık Tectonic Slice.

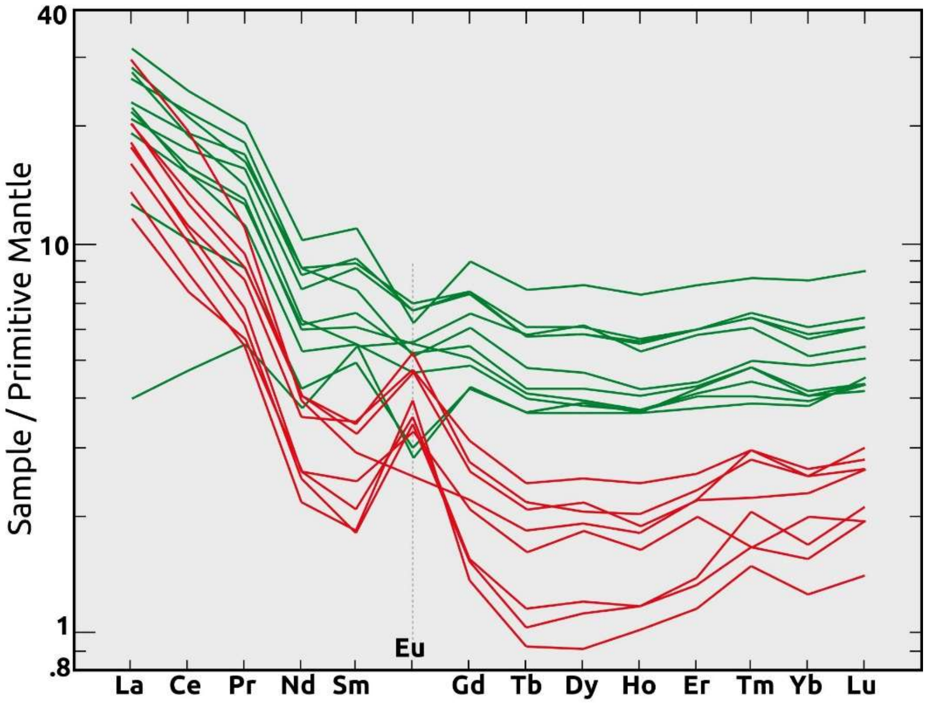

Figure 3.5 Spider diagram of the Kavacık granite, Spider Diagram is nomalized to the Primitive Mantle Rocks (McDonough & Sun, 1995)

CHAPTER FOUR
GEOCHRONOLOGY

In the study area, zircons obtained from 2 granite samples representing Kavacık granite were aged by ICP-MS LA[1] method. In this part of the report, the sample preparation for radiometric age determination, cathodoluminescence (CL) images zircon and the obtained age determination results will be given.

4.1 Mineral (Zircon) Enrichment

The zircon minerals used for radiogenic age determination have been made ready for analysis by selecting them according to their morphology and observable crystal properties in a stereomicroscope. Its their crystall properties identified by CL before analysis were examined and points will make age determination were identified. The CL images and analysis points obtained from the zircons are shown in Figure 4.1.

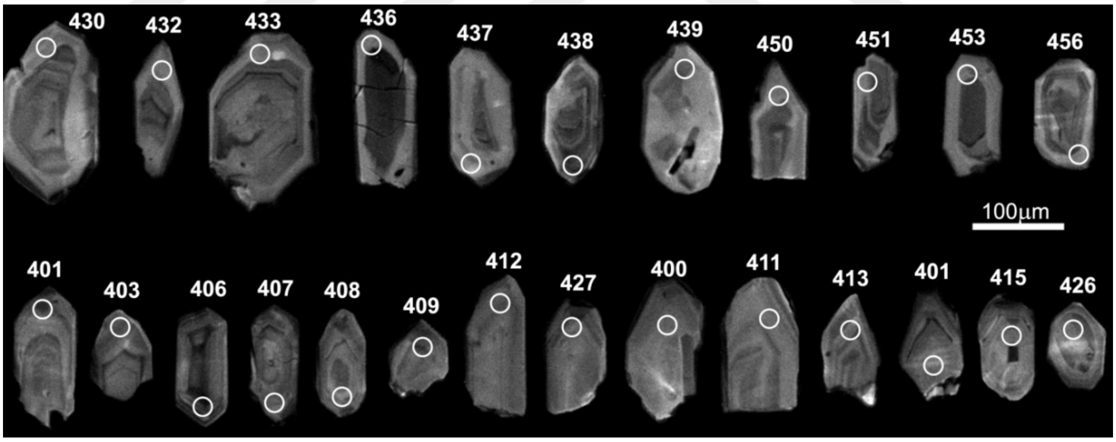

Figure 4.1 CL images and analysis points of zircons of Kavacık granite

4.2 CL Images and ICP-MS LA Analytical Method

The separated zircon grains were selected with the help of a stereomicroscope and put into the epoxy in the appropriate mechanism, making them suitable for both CL and ICP-MS LA analyzes. Cathodoluminescence (CL) images were obtained in the Earth Sciences Institute of Mainz University (Germany) with the help of a Jeol JXA-

8900RL electron microscope. In the same department, U, Th and Pb isotope measurements were performed with the ESINWR193 ArF laser system, which is capable of producing 193 nm wavelength laser paired with Agilent 7500ce quadrupole ICP-MS. The first data obtained is calculated by GLITTER 4.4.1 program and it is made suitable to the table to be created in excel. Concordia diagrams are drawn in the ISOPLOT program as the result of analytical calculations made in Excel.

4.3 Analytical Results

As stated above, analytical ages were calculated from 2 samples of Kavacık Granite using CL images (Figure 4.1) and ICP-MS Laser Ablation. According to this, the zircons of Kavacık granite are observed mostly self-shaped and they are in the range of approximately 75-125 µm. The CL images of the zircons of Kavacık granite show that they are all magmatic source (Figure 4.1). Zircons generally consist of smooth magmatic envelopes that unaffected by hydrothermal alteration. Ages of some zircons of Kavacık granites vary from 278 to 259 Ma and concordant ages of the majority of zircons range between 224-230 Ma (Figure 4.2).

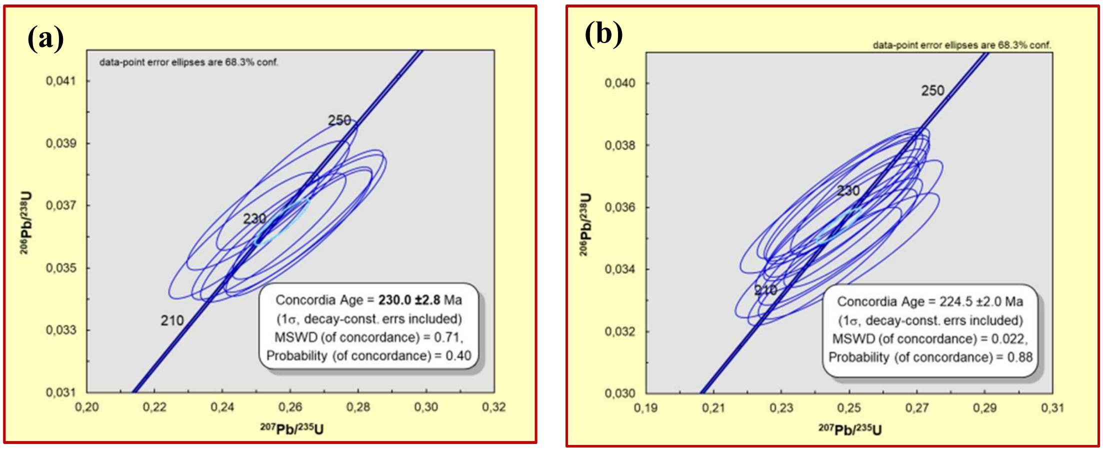

Figure 4.2 Concordia diagrams of isotopic measurement of zircons separated from Kavacık granite (a) KAV-6 and (b) KG-1 number (up)

Table 4.1 ICP-MS LA radiometric age analysis results of Kavacık Granite

Kavacık Granite			**İsotope ratios**						**Age (My)**				
ÖRNEK	**Analiz No**	**$^{207}Pb/^{206}Pb$**	**1σ**	**$^{207}Pb/^{235}U$**	**1σ**	**$^{206}Pb/^{238}U$**	**1σ**	**$^{207}Pb/^{235}U$**	**1σ**	**$^{206}Pb/^{238}U$**	**1σ**		
KAV6	430	0.0490	0.0029	0.2489	0.0157	0.0358	0.0014	226	13	227	8	**224.5 ±2.0 My**	
	432	0.0484	0.0025	0.2473	0.0148	0.0363	0.0014	224	12	230	8	**224.5 ±2.0 My**	
	433	0.0515	0.0029	0.2428	0.0149	0.0341	0.0013	221	12	216	8	**224.5 ±2.0 My**	
	436	0.0499	0.0023	0.2522	0.0129	0.0365	0.0013	228	10	231	8	**224.5 ±2.0 My**	
	437	0.0523	0.0027	0.2541	0.0154	0.0355	0.0014	230	13	225	8	**224.5 ±2.0 My**	
	438	0.0514	0.0032	0.2474	0.0159	0.0349	0.0014	224	13	221	8	**224.5 ±2.0 My**	
	439	0.0497	0.0029	0.2465	0.0160	0.0353	0.0014	224	13	224	9	**224.5 ±2.0 My**	
	450	0.0521	0.0034	0.2498	0.0176	0.0344	0.0013	226	14	218	8	**224.5 ±2.0 My**	
	451	0.0506	0.0034	0.2432	0.0177	0.0345	0.0014	221	14	219	9	**224.5 ±2.0 My**	
	453	0.0496	0.0035	0.2458	0.0184	0.0361	0.0014	223	15	228	9	**224.5 ±2.0 My**	
	456	0.0507	0.0028	0.2475	0.0150	0.0356	0.0013	225	12	226	8	**224.5 ±2.0 My**	
	457	0.0502	0.0029	0.2494	0.0159	0.0363	0.0014	226	13	230	9	**224.5 ±2.0 My**	
	458	0.0501	0.0031	0.2483	0.0168	0.0365	0.0014	225	14	231	9	**224.5 ±2.0 My**	
	431	0.0557	0.0038	0.3291	0.0231	0.0427	0.0017	289	18	270	10	**259.0 ±20 My**	
	452	0.0520	0.0028	0.3095	0.0173	0.0435	0.0016	274	13	275	10	**259.0 ±20 My**	
	454	0.0560	0.0039	0.3151	0.0234	0.0411	0.0017	278	18	260	10	**259.0 ±20 My**	
KG1	402	0.0499	0.0027	0.2463	0.0146	0.0361	0.0013	224	12	228	8	**230.0 ±2.8 My**	
	403	0.0501	0.0028	0.2535	0.0157	0.0370	0.0014	229	13	234	9	**230.0 ±2.8 My**	
	406	0.0498	0.0023	0.2590	0.0137	0.0377	0.0014	234	11	238	9	**230.0 ±2.8 My**	
	407	0.0532	0.0026	0.2625	0.0142	0.0361	0.0013	237	11	229	8	**230.0 ±2.8 My**	
	408	0.0524	0.0034	0.2609	0.0181	0.0363	0.0016	235	15	230	10	**230.0 ±2.8 My**	
	409	0.0529	0.0027	0.2651	0.0147	0.0367	0.0014	239	12	232	9	**230.0 ±2.8 My**	
	412	0.0513	0.0027	0.2537	0.0150	0.0360	0.0013	230	12	228	8	**230.0 ±2.8 My**	
	427	0.0521	0.0026	0.2622	0.0145	0.0362	0.0013	236	12	229	8	**230.0 ±2.8 My**	
	400	0.0501	0.0034	0.2774	0.0192	0.0395	0.0015	249	15	250	9	**246.2 ±4.4 My**	
	411	0.0516	0.0035	0.2803	0.0204	0.0394	0.0015	251	16	249	9	**246.2 ±4.4 My**	
	413	0.0530	0.0034	0.2871	0.0192	0.0390	0.0015	256	15	247	9	**246.2 ±4.4 My**	
	401	0.0504	0.0035	0.3077	0.0224	0.0445	0.0017	272	17	280	10	**278 ±5.1 My**	
	415	0.0517	0.0030	0.3054	0.0183	0.0427	0.0016	271	14	270	10	**278 ±5.1 My**	
	426	0.0526	0.0037	0.3211	0.0212	0.0445	0.0017	283	16	281	11	**278 ±5.1 My**	

CHAPTER FIVE
STRUCTURAL GEOLOGY

In this chapter, the mesoscopic and microscopic structural elements in the Kayabaşı, Boytaş, Kavacık and Çatalkaya tectonic slices of the Bornova melange are described. The four tectonic slices were strongly brittly and semi-brittly sheared and show a prominent foliation with linear fabric. All tectonic slices expose along NE-SW direction and moderately dip to NW (Plate I). The primary contact relationship of the rocks in the tectonic slices were obliterated due to the high strain. Not only the boundries of the tectonic slices are represented by shear zones but also the most of their primary structures were obliterated by high strain.

Sandstones-shales, mafic volcanics and serpentinites in the Bornova Melange show anastomosing foliation which diagnosed by intersection of shear fractures (Figures 5.1, 5.2, 5.12 a,b, 5.13 a,b). Along the contact zone serpentinites show a prominent anastomosing foliation (Figure 5.1).

Figure 5.1 Strongly foliated serpantinites in the Kayabaşı Tectonic Slice close to the contact to the Kavacık Tectonic Slice [0498840; 4241643] 817 m. (Personal archive, 2016)

Figure 5.2 Strongly foliated sandstone-shale complex in the Kavacık Tectonic Slice [0498822; 4241687] 813 m. (Personal archive, 2016)

Thin section studies show that the sandstones contain elongated and oriented quartz and feldspar grains in microlithons (Figure 5.3). Around these grains the discontinuous dark seams. Cleavage domains and mica beard around grains indicate a rough foliation. The mica beards are composed of tiny sericites and quartz. In the high strain zones, the continuous foliations in phyllites and serpenites are also observed (Figure 5.4, 5.5).

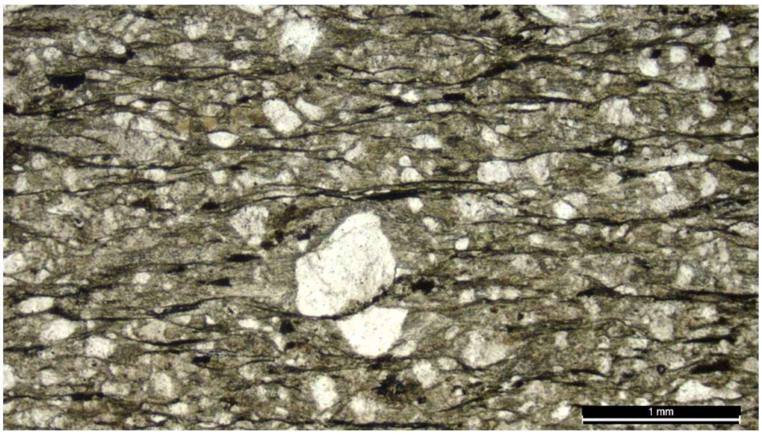

Figure 5.3 Range foliation in sandstone of the Kavacık Tectonic Slice [0497449; 4241247] 826 m. Around the coarse grained quartzs and feldspars in microlithons the micabeards composed of tiny serisite and chlorite crystals are seen (white arrows). Discontinuous black seams forms the range foliation (Personal archive, 2018)

The linear fabrics as in the study area measured are as follows:

- Stretching lineation
- Long axis of oriented pebbles (deformed pebbles)
- Boudins
- Crenulation axis
- Axis of mesoscopic folds
- Pencil structures
- Fibrous minerals filled in tension gashes
- Slicken lines
- Brittle structures

The stretching lineation is decribed by the linear arrangement of grains on the foliation surfaces (Figure 5.4 a,b) along high strain shear zones located to the contacts of the tectonic slices. Crenulation and tight, mesoscopic folds are found in the fine-grained parts of Kavacık Tectonic Slice to the southeast of Kavacık village (Plate 1).

Pencil structures and boudins accompany tightly folded sandstones – shales alternation both in Kayabaşı and Çatalkaya Tectonic Slices (Figure 5.6 a). Fibrous quartz and chlorite crystals filled the tension gashes are found in the leucocratic parts of the Kavacık Tectonic Slice (Figure 5.6 b).

Figure 5.4 Stretching lineation in the Kavacık Tectonic Slice and Kayabaşı Tectonic Slice (a) Along the foliation plane in recrystallized limestones along the contact between the Kavacık and Kayabaşı Tectonic slices [0497243;4239982] 458 m. (b) Stretching lineation in strongly foliated mudstones in the Kavacık Tectonic Slice (Personal archive, 2016)

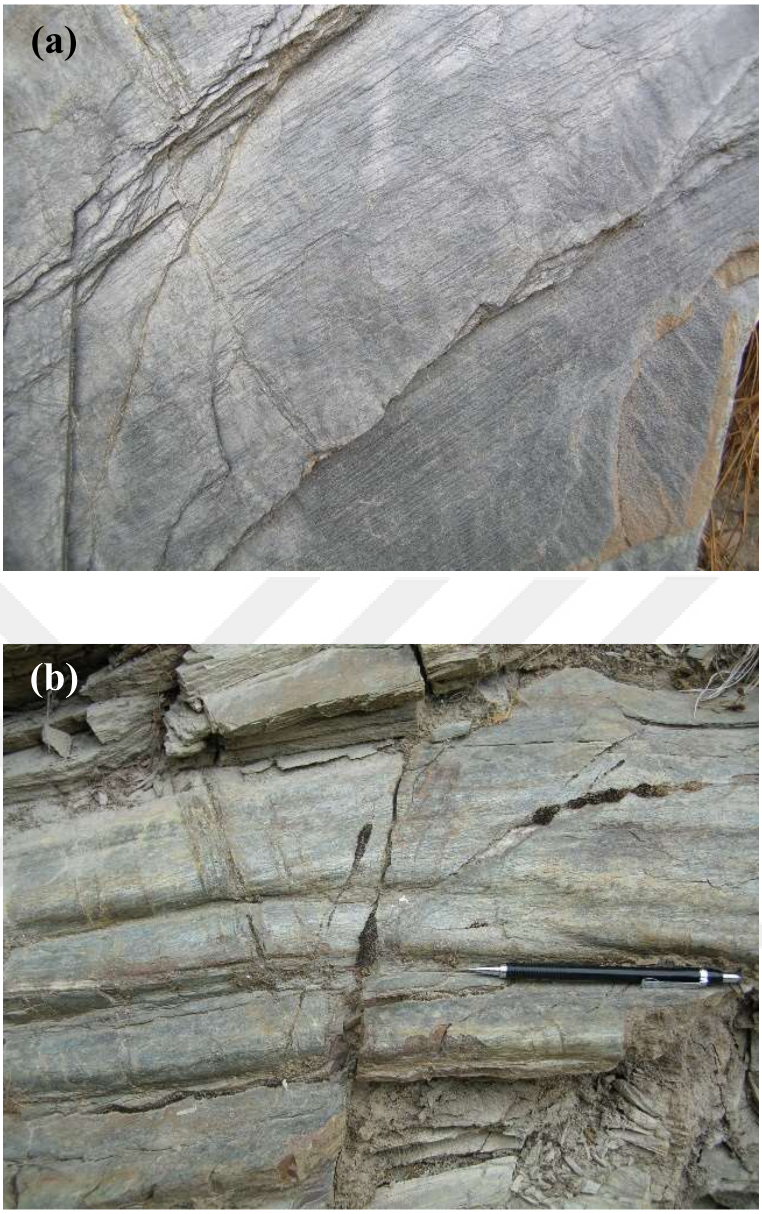

Figure 5.5 Crenulation lineation and mesoscopic folds in the Kavacık Tectonic Slice. (a) Prominent crenulation axis in metapelites [0500165; 4242962] 913 m. (b) Mesoscopic folds in sandstone-shale alternation [0500213; 4242727] 845m. (Personal archive, 2017)

Figure 5.6 (a) Pencil structures in sandstone – shale alternations in the Çatalkaya Tectonic Slice. [0500127; 4242343] 848 m. (b) Fibrous quartz and crystals in tension gashes in the granits of the Kayabaşı Tectonic Slice [0500065; 4242212] 832 m. (Personal archive, 2016)

In the study area, Kavacık Tectonic Slice expose in NE – SW direction between Balçova and Kavacık Village (Plate I). Petrographic analysis reveal that the Kavacık granite show both cataclastic and mylonitic textures (Figure 5.7). In the internal part of the Kavacık Tectonic Slice, the low strain zones expose cataclastic texture marked by disintegrated quartz and feldspar crystals in microscopic scale (Figure 5.7 a). However, toward the contact zone Kavacık granite exhibits mylonitic texture diagnosed by oriented mica matrix and elongated quartz and feldspar grains (Figure 5.7 b,c).

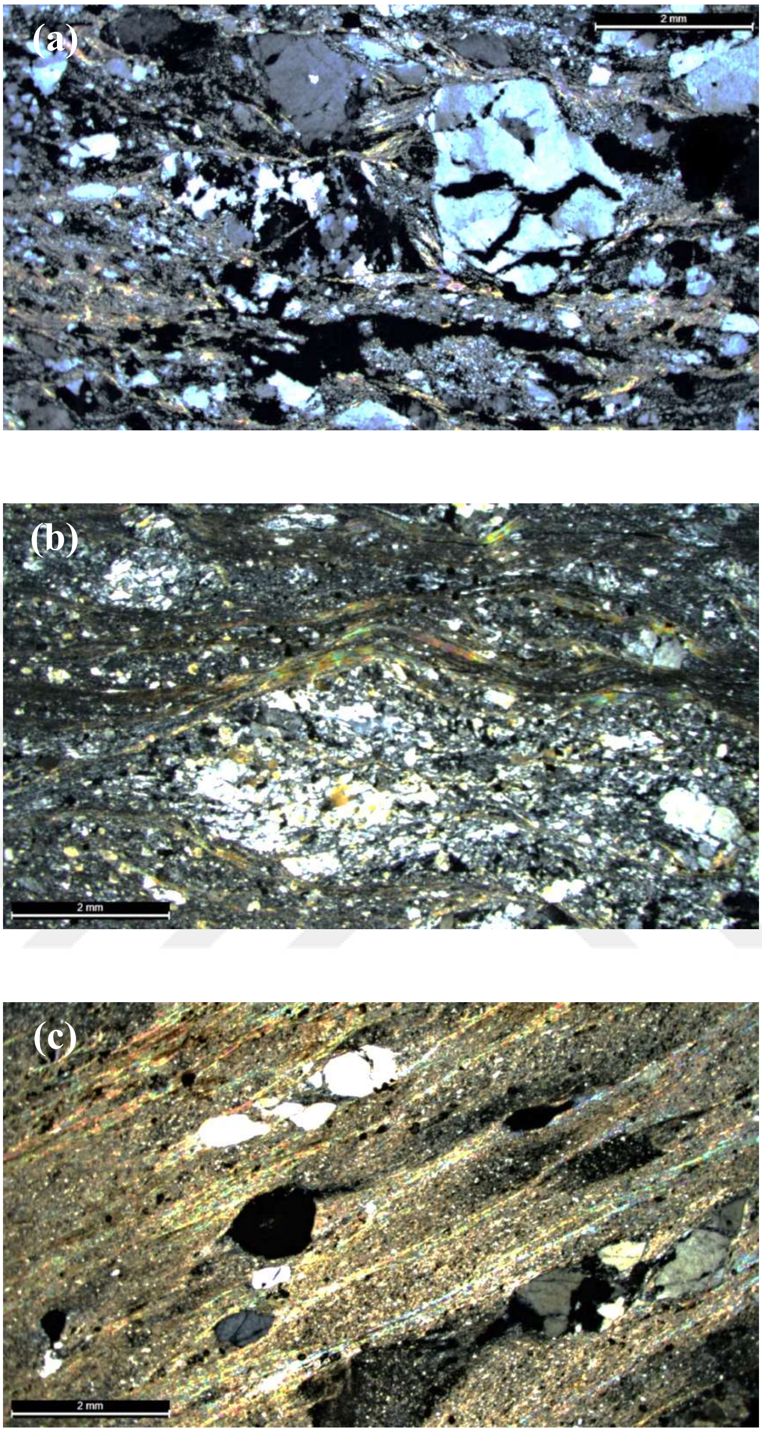

Figure 5.7 Textures showing the variation of the strain in the granite of the Kayabaşı Tectonic Slice. (a) Cataclastic texture in leucogranite of the Kayabaşı Tectonic Slice. (b) Disintegrated quartz and feldspar crystals. A newly formed foliation plane is marked by preffered orientation of micas. (c)strongly foliated granite. Foliation is marked by parallel orientation of micas and flattened quartz and feldspar porphyroclatic. All microphotograps from the samples taken from the contact between the Kavacık Tectonic Slice and Kayabaşı Tectonic Slice (Personal archive, 2017)

In the mesoscopic scale the Kavacık Tectonic Slices was brittly sheared. Shear fractures are seen penetratively thoughout the Kavacık granite (Figure 5.11). Shear fractures are also common in the Kayabaşı tectonic slice. These shear fractures separate mafic volcanics, serpentinites and sandstone-shales. Along these fractures brecciation reach up to 50 cm thick zones (Figure 5.11 c).

Turbiditic sandstone – shale alterations in the Kayabaşı and Çatalkaya Tectonic Slices were obliterated into sandstone – shale complex diagnosed by shear fractures that form anastomosing foliation in mesoscopic scale (Figure 5.2., 5.3).

However, in oriented thin sections of sandstones show ductile deformation marked by cleavage and microlithons (Figure 5.8). In Figure 5.8.a cleavage domains are represented by almost continuous dark seems composed of tiny phyllosilicates and residue from the dissolution. In the microlithons, between cleavage domains, the quartz and feldspar grains oriented parallel and subparallel to the cleavage domains.

Besides these, around the grains in the microlithons, the mica beards composed of sericite, chlorite and quartz crystals are clearly seen (Figure 5.8 b) white arrows. The cleavage domains and microlitons indicate that the main deformation mechanism was the pressure solution in the sandstones in both the Kayabaşı and Çatalkaya Tectonic Slices.

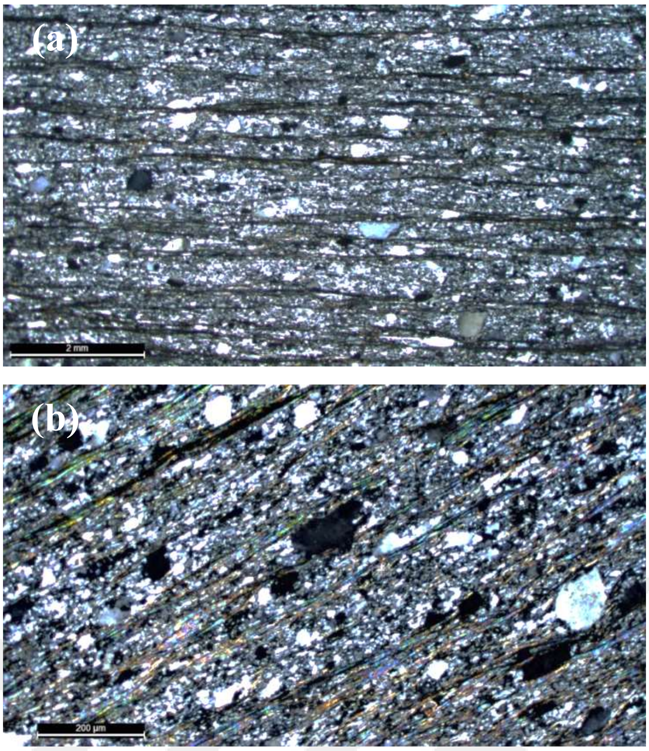

Figure 5.8 Photomicrographs showing rough foliation in sandstone located to the contact between Kayabaşı Tectonic Slice and Çatalkaya Tectonic Slices. (a) Rough foliation is diagnosed by both discontinuous dark seams and flattened, quartz and feldspar grain in microlithons. (b) Closer view of rough foliation also show micabeards around grains (whit arrows) [0497800; 4244000] 770 m. (Personal archive, 2018)

In the study area, both in the internal parts of the tectonic slices and specially along their shared contacts, the mesoscopic structures were measured. The contour diagrams of foliation and linear fabrics measured in the four tectonic slices are presented in Figures 5.9 and 5.10. Figure 5.9 shows that the foliation strikes NS direction and moderately dip to W. The linear fabric along the foliation surface trends boths N and NE, and shallowly plung N, S, NE and SW.

The asymmetric structures both outrops and thin section oriented perpendicular to the foliation and parallel to the associated linear fabric were used to kinematic analysis.

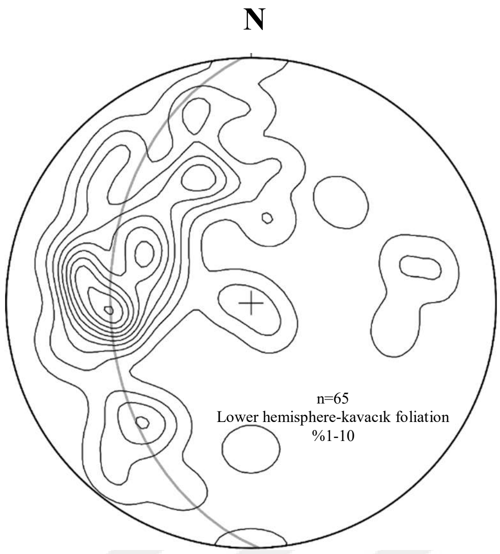

Figure 5.9 Contour diagram of foliation measured in tectonic slices of the study area. The diagram shows that mean foliation strikes N-S and moderately dips to W.

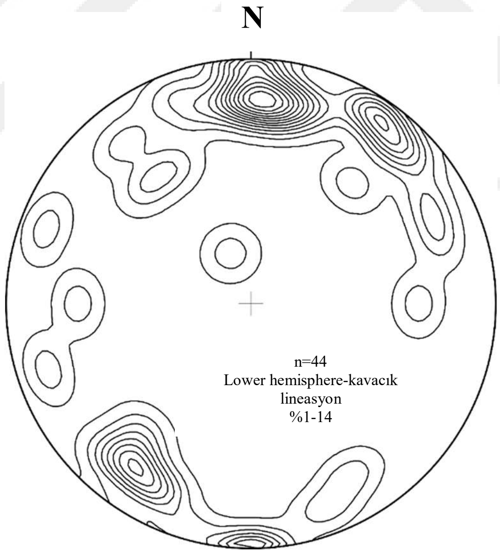

Figure 5.10 Contour diagram of the linear fabric measured in tectonic slices of the study area. Linear fabric along the foliation planes shows a trend N and NE, and plung to N, S, NE and SW. Relation between foliation and associated linear fabric clearly show a strike parallel movement

Figure 5.12.a shows quartz sigmoid with top-to-the southwest sense of shear in the Çatalkaya tectonic slices. Asymmetric boudins of sandstone bed also indicate a top-to-the southwest sense of shear in the same tectonic slice (Figure 5.12.b). In the Kayabaşı tectonic slice a quarter fold marked by thin limestone layer (Figure 5.12.c)

and eu-echelon tension gashes (Figure 5.12.d) in the sandstones show top-to-the southwest sense of shear.

Figure 5.11 Brittle shear zones in the study area. (a) Shear zone between serpanitinites (below) and mafic volcanic rocks in the Kavacık Tectonic Slice [0500517; 4242080] 888 m. (b,c,d) Mesocopic

brittle shear zones in the granites of Kayabaşı Tectonic Slice [0499643; 4243285] 846 m. (Personal archive, 2016)

Figure 5.12 Shear sense indicators in the study area. All views are parallel to the linear fabric and perpendicular foliation plane. (a) Quartz sigmoid in strongly strainedsandstone-shale in the Çatalkaya Tectonic Slices [0499363; 4245009] 297 m. (b) Asymmetric boundinage of sandstone layer in the Çatalkaya Tectonic Slice [0499363; 4245009] 297 m. (c) A quarter fold of limestone

sense in sandstone – shale alternation in the Kavacık Tectonic Slice [0498822; 4240975] 772 m. (d) En-Eechelon tension gashes in the sandstones of the Kavacık Tectonic Slice [0497156; 4240070] 501 m. All asymmetric structures point a top-to-the S or SW sense of shear (Personal archive, 2016)

In a shear zone the sandstones withs sigmoidal foliation in the Çatalkaya tectonic slice show top-to-the southwest (Figure 5.13).

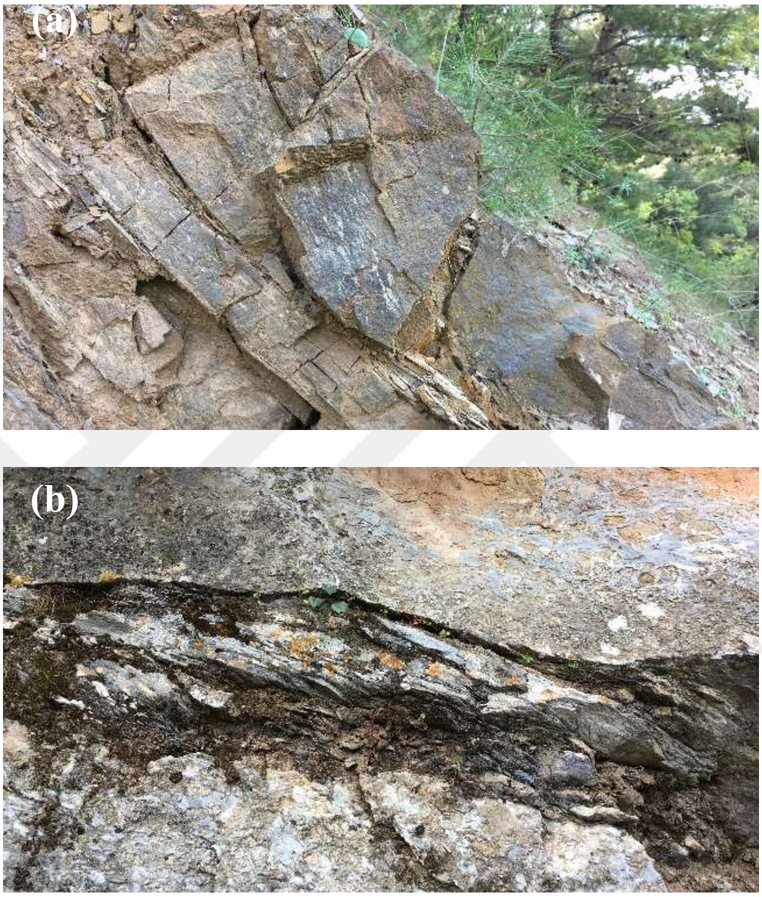

Figure 5.13 Shear sense indicators in the Çatalkaya Tectonic Slice. Both views are parallel to the linear fabric and poprudicular to the foliation (a) sigmoidal foliation in sandstones in shear zones. (b) Imbrication of a thin layer of recrystallized limsedtone in shear zones between two massive limestone beds. Sigmoidal foliation in a and imbrication in b both show a top-to-the S and SW sense of shear [0499360; 4245010] 298 m. (Personal archive, 2017)

Imbrication of a thin limeston layer also show top-to-the southwest sense of movement. Kink bands in the Kayabaşı tectonic slice also indicate top-to-the south and southwest sense of movement (Figure 5.14 a,b).

Figure 5.14 Asymetric kink bands in the metapelitic parts of the Kayabaşı Tectonic Slice (a) and Çatalkaya Tectonic Slice (b) Both asymmetric kinks show a top-to-the S and SW sense of movement in the study area [0498840; 4241643] 817 m. (Personal archive, 2016)

The contact between the Kavacık and Çatalkaya tectonic slices, are represented by continuous foliation with stretching lineation in high strain zones toward southwest of the study area and fault plane with slickenlines in brittle zone toward northeast of the study area (Figure 5.15).

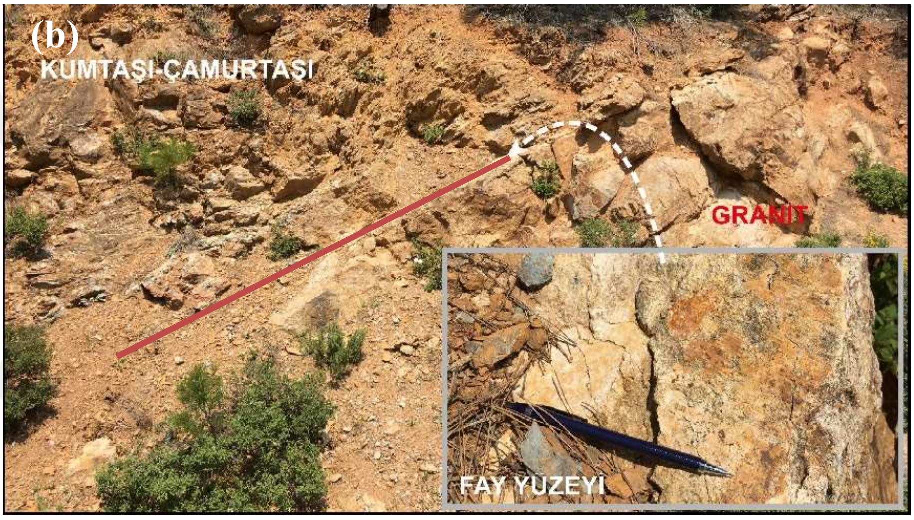

Figure 5.15. Two views along the contact between the Kavacık and Çatalkaya Tectonic Slices. (a) Stretching lineation in the upper contact zone of the Kayabaşı Tectonic slice with the Çatalkaya Tectonic Slice [0498039; 4244066] 741 m. Brittle fault zone between granites of the Kayabaşı Tectonic Slice and the sandstone-shale of the Çatalkaya Tectonic Slice. Sandstone-shale complex form the hanging wall and granites form footwall [0500830; 4245251] 484 m. in set photo show slickenlines with a NE – SW trendon the fault plane. Small rake angles in both photograps clearly a strike-slip dominant sense of movement (Personal archive, 2016)

- **Relation of Kavacık Granite with Efemçukuru Gold Deposit and Balçova Geothermal Area**

The Efemçukuru gold deposit in the tectonic slice underlying the Kavacık Tectonic Slice is located in a NW-SE striking tension gash. In previous studies, it is suggested that it is related Miocene rhyolitic volcanism. But volume of rhyolitic volcanites is very small and they do not show any alteration zone. The formation of this gold deposit may be associated with Kavacık granite and the temporal relationship should be investigated by making Ar-Ar geochronology *[hornfelsic rocks located aroun gold deposit, amphibole crystals and gold vein contain K-feldspar, which are suitable only for Ar-Ar geochronology study]* from the metamorphic rock in which the mineralization is located. The result obtained here will reveal the temporal relationship of Kavacık granite with gold mineralization. After that, spatial relation can be solved making with a geological map which covers both the Kavacık granite and the mineralization area.

Due to the age of Kavacık granite (range 278-235 Ma) and structural position (tectonic slice), it is not possible to be considered as a heating source for the Balçova Geothermal system. It is not possible to protect the temperature of a magmatic mass, formed in the Early Permian-Early Triassic age range, during this period. Furthermore, to be as a thin tectonic slice in the Bornova Melange suggests that it traveled long distances from its origin to a low temperature subduction zone. With these properties, Kavacık granite shows that it has lost its heat source property for a geothermal system long time ago.

CHAPTER SIX
CONCLUSIONS

The following results were obtained by making a geological map of Kavacık granite expansion between Kavacık Village and Balçova (İzmir):

- Geochemistry and geochronological characteristics of the Kavacık granite in the Bornova Melange are described.

- Kavacık holocrystalline forms fabric and its composition is distributed between granite and diorite.

- The geologic features and zircon crystallization ages of Kavacık granite in İzmir-Ankara Zone have been investigated by U-Pb isotope analysis. The U-Pb zircon laser ablation ages were obtained from Kavacık granite ranging from 224.5 ± 2.0 Ma and 230.0 ± 2.8 Ma.

- The age of Kavacık Granite is similar to the ages previously determined in Karaburun Peninsula (Karaburun Granite) and Menderes Massif (Ödemiş-Kiraz Submassive).

- Kavacık granite is as a tectonic slice extending approximately in NE-SW direction (Plate 1).

- The geochemical properties of Kavacık granite indicate an ensimatic arc granitoid with I-type and subalcaline characterized and determine that an ensimatic arc that existed in the Early Permian-Early Triassic time interval included in the İzmir-Ankara suture zone in the Late Cretaceous-Late Paleocene range.

REFERENCES

Akartuna, M. (1962). On the geology of İzmir-Torbalı-Seferihisar-Urla district. *Maden Tetkik Arama Bülteni.*, *59,* 1-18.

Başarır, E. & Konuk, Y.T. (1981). Gümüldür yöresinin kristalin temeli ve allokton birimleri. *Türkiye Jeoloji Kurultayı Bülteni,* 1-6.

Brinkmann, R., & İzdar, E. (1971). *Excursions near İzmir and Manisa*. In "Geology and History of Turkey", ed. A.S. Campbell, *Petroleum Exploration Society of Libya, Tripoli*., 505-508.

Brinkmann, R., Rendel, B., & Trick, P. (1967). Pelagische Trias bei İzmir. *Ege Üniversitesi Fen Fakültesi İlmi Raporlar Serisi*, No. 37.

Brinkmann, R., Flügel, E., & Jacobshagen (1972). Trias, Jura und Unterkreide der Halbinsel Karaburun (West-Anatolien). *Geology et Paleont*ology, *6*, 139-150.

Erdoğan, B., (1990). İzmir-Ankara Zonu ile Karaburun Kuşağının tektonik ilişkisi. *Maden Tetkik Arama Dergisi, 110*, 1-15.

Erdoğan, B. (1990). İzmir-Ankara Zonu'nun, İzmir ile Seferihisar arasındaki bölgede stratigrafik özellikleri & tektonik evrimi. *Türkiye Petrol Jeologları Derneği Bülteni*, *2*, 1-20.

Erdoğan, B., Altıner, D., Güngör, T., & Özer, S. (1990). Karaburun Yarımadasının stratigrafisi. *Maden Tetkik Arama Dergisi*, *111*, 1-23.

Floyd, P.A., 1993. Geochemical discrimination and petrogenesis of alkalic basalt sequences in part of the Ankara melange, central Turkey. *Journal of the Geological Society of London, 150*, 541-550.

Gessner, K., Ring, U., Johnson, C., Hetzel, R., Passchier, C.W., & Güngör, T. (2001a). How to resist subduction: evidence for large-scale out of sequence thrusting during Eocene collision in western Turkey. *Journal of the Geological Society London, 158*, 769-784.

Irvine, T. N. & Baragar, W.R.A., A., (1971), Guide to the chemical classification of the comman volcanic rocks, can. *Journal Earth Science, 8*, 543-548.

Konuk, Y.T. (1977). On the age of the Bornova Flysh. *Ege Üniversitesi Fen Fakültesi Dergisi, Serie B 1*, 65-73.

Okay, A.I., Altıner, D. (2007). A condensed Mesozoic section in the Bornova Flysch Zone: A fragment of the Anatolide–Tauride carbonate platform. *Turkish Journal of Earth Sciences 16,* 257–279.

Oyman, T., Minareci, F., & Piskin O. (2003). Efemcukuru B-rich epithermal gold deposit (Izmir, Turkey), *in Ore Geology Reviews*, 35-53.

Öngür, T. (1972). İzmir Urla Jeotermal araştırma sahasına ilişkin jeolojik rapor. *Maden Tetkik Arama Rapor no.4835 (yayımlanmamış),* Ankara.

Özer, S., & İrtem, O. (1982) Işıklar-Altındağ (Bornova- İzmir) alanı Üst Kretase kireçtaşlarının jeolojik konumu, stratigrafisi & fasiyes özellikleri. *Türkiye Jeoloji Kurumu Bülteni, 25*, 41-47.

Okay, A.İ., İşintek, İ., Altıner, D., Özkan-Altıner, S., Okay, N. (2012). An olistostrome-mélange belt formed along a suture: Bornova Flysch zone, western Turkey. *Tectonophysics*, *568*, 282-295.

Pearce, J. A., Harris, N.B.W., & Tındle, A.G., 1984, Trace element discrimination diagrams for the tectonic inter pratation of granitic rocks: *Journal of Petrology., 25*, 956- 983.

Pearce, J.A., (1975). Basalt geochemistry used to investigate past tectonic environments on Cyprus. *Tectonophysics*, *25*, 41-67.

Pearce, J.A., (1983). The role of sub-continental lithosphere in magma genesis at destructive plate margins. In: C.J. Hawkesworth, and M.J. Norry (eds), *Continental Basalts and Mantle Xenoliths,* 230-249.

Pearce, J.A., and Cann, J.R., 1973. Tectonic setting of basic volcanic rocks determined using trace element analysis. *Earth and Planetary Science Letters, 19*, 290-300.

Pearce, J.A., and Norry, M., 1979. Petrogenetic implications of Ti, Zr, Y and Nb variations in volcanic rocks. *Contributions to Mineralogy and Petrology, 69*, 33-47.

Poisson, A., & Şahinci, A. (1988). La serie mèsozoique de Kemalpaşa et le flysh palèocene de Izmir ou nordo, uest du Menderes (Anatolie occidentale, Turquie). Un Jalon du microcontinent taurique. *Comptes rendus de I'Academie des Sciences, Paris, 307*, 1075-1080.

Ring at all. (1999). The Menderes Massif of western Turkey and cycladic massif in Agean-do taheyreally correlate? *Journal of the Geological Society London, 156*, 3-6.

Sarı, B. (2013). Late Maastrichtian-Late Palaeocene Planktic Foraminiferal Biostratigraphy of the Matrix of the Bornova Flysch Zone around Bornova (İzmir, Western Anatolia, Turkey). *Turkish Journal of Earth Sciences (Turkish Journal Earth Sciences), 22*(1), 143-171.

Winchester, J.A., & Floyd, P.A., 1977. Geochemical discrimination of different magma series and their differentiation products using immobile elements. *Chemical Geology, 20*, 325-343.

Wood, D.A., 1979. Variably – veined sub – oceanic upper mantle : Genetic significance for mid –ocean ridge basalts from geochemical evidence. *Geology, 7*, 499-503.

APPENDICES

Appendix 1:

Table 1. Kavacık Granitoids Geochemistry Results

	GR-1	GR-2	GR-5	GR-6	GR-10	GR-11	KAV-1	KAV-2	KAV-3	KAV-4	KAV-5	KAV-6	KAV-7	Ma-3	Ma-4	Ma-7	Ma-8	Ma-9	Ma-12	Ma-13
SiO2	74,3	71,4	70,1	71,9	62,7	68	75,68	69,52	47,41	66,81	56,93	75,39	62,33	55,9	55,6	55	54,8	59,4	56,4	57,8
Al2O3	12,85	12,2	13,3	13,35	16,65	14,1	12,97	15,07	16,16	16,15	16,73	12,24	15,95	15,45	15,8	16,7	17,25	15,1	15,85	15,95
Fe2O3	1,64	3,86	3,72	3,5	5,97	4,47	2,06	3,53	8,32	3,85	8,44	2,3	6,81	8,58	10,7	10	7,64	8,42	8,33	9,5
MgO	0,25	0,69	1,21	1,42	1,78	1,66	0,85	0,9	8,44	1,36	4,18	0,85	2,66	4,94	3,13	4,56	4,53	3,37	5,04	3,49
CaO	2,16	4,19	2,96	2,12	4,43	2,9	0,6	2,7	10,82	3	4,78	2,1	3,27	4,65	6,13	7,03	4,09	4,49	5,54	5,17
Na2O	5,86	3,69	3,2	3,74	3,07	4,58	4,84	4,83	3,36	3,3	2,99	2,9	2,71	3,79	2,7	3,09	4,2	3,29	3,03	2,9
K2O	0,24	0,48	1,35	1,37	1,88	0,73	1,24	0,79	0,06	2,43	1,57	1,72	1,95	1,26	1,29	1,14	1,94	1,09	1,4	0,95
TiO2	0,09	0,3	0,33	0,31	0,54	0,39	0,16	0,32	0,93	0,29	0,71	0,16	0,51	0,66	0,89	0,66	0,43	0,79	0,61	0,72
P2O5	0,02	0,06	0,07	0,06	0,13	0,08	0,04	0,08	0,07	0,07	0,1	0,03	0,09	0,09	0,13	0,07	0,06	0,1	0,08	0,09
MnO	0,03	0,06	0,06	0,05	0,1	0,07	0,03	0,06	0,14	0,07	0,17	0,04	0,11	0,17	0,2	0,19	0,13	0,16	0,17	0,18
Cr2O3	<0.01	<0.01	<0.01	<0.01	<0.01	<0.01	<0.002	<0.002	0,058	<0.002	<0.002	<0.002	0,002	<0.01	<0.01	<0.01	0,01	<0.01	<0.01	<0.01
LOI	1,07	1,6	2,1	2,11	3,3	2,51	1,3	1,9	3,9	2,3	3,1	1,8	3,2	2,94	3,13	3,12	5,96	4,6	3,55	3,08
Sum	98,54	98,57	98,46	100	100,62	99,54	99,76	99,78	99,72	99,71	99,73	99,58	99,67	98,48	99,76	101,62	101,1	100,86	100,05	99,88
Mo	2	<2	2	<2	<2	<2	<0.1	0,1	<0.1	<0.1	<0.1	0,1	<0.1	<2	<2	<2	<2	<2	<2	<2
Cu	7	14	13	8	21	50	1,5	2,1	30,3	60	35,8	11,6	565,4	7	18	31	<5	14	11	73
Pb	<5	5	<5	<5	6	<5	2	1	0,1	1,5	1,6	1,5	1,8	<5	6	5	<5	6	6	6
Zn	10	26	58	31	63	42	18	29	31	29	58	18	80	75	99	90	71	89	80	87
Ni	5	5	7	8	6	6	1,5	0,8	100,8	2,3	3,9	1,8	2,8	7	5	9	14	5	12	6
Tl	<0.1	<0.1	<0.1	<0.1	<0.1	<0.1	<0.1	<0.1	<0.1	<0.1	<0.1	<0.1	<0.1	<0.5	<0.5	<0.5	<0.5	<0.5	<0.5	<0.5
Co	41,7	31,9	37,3	34	33,8	46,3	146,9	94,7	80,8	127,1	85,4	235,5	98	31,6	34,5	43,1	32,1	28,4	30,7	29,9
Cs	0,13	0,19	0,58	0,56	2,35	0,91	0,8	0,7	0,1	2,3	1,5	0,7	1,6	0,69	0,54	0,63	1,61	1,2	1,7	1,45
Ga	10,8	13,3	12,9	12,8	17,3	13,5	9,7	11,9	11,3	12,6	14	8,3	14,5	15,6	18,5	17,6	15,7	17,3	16,7	17,5
Hf	2,1	2,9	3,4	2,2	4,5	2,6	2,7	4,6	1,9	2,9	2	1,8	1,8	1,8	2,1	2,4	3	2,5	2	2,2
Nb	3,9	2,3	2,9	2,5	4,8	3,5	5,5	7	1,4	2,7	5,7	2,5	4,1	4	4,7	5,5	2,7	5,4	3,7	5,6
Rb	4,8	13	34,4	37,1	55	23,3	32,4	17,9	1,2	60	44,6	32,2	43,9	42	37,1	30,8	59,5	34,9	46,2	30
Sn	<1	<1	1	1	1	1	1	1	<1	<1	<1	2	<1	1	1	1	1	1	1	1
Sr	135	205	182	139,5	241	212	92,4	150,4	191,8	193,9	185,7	119,7	157,2	147	222	206	63,2	172,5	202	242
Ta	0,7	0,3	0,4	0,3	0,4	0,3	0,5	0,6	0,1	0,3	0,5	0,4	0,4	0,3	0,4	0,4	0,3	0,5	0,4	0,4
Th	12,3	5,5	4,89	3,89	3,91	3,39	7,2	5,9	<0.2	3,9	4,2	3	3,8	3,83	3,01	3,8	3,52	4,57	4,41	3,01
U	2,02	0,79	1,27	1,46	0,86	1,1	1,5	1,3	<0.1	0,7	0,7	0,9	0,7	0,79	0,71	1,11	0,87	0,96	0,8	0,72
V	15	49	40	47	91	83	14	21	217	48	240	33	140	211	221	242	148	200	193	234
W	523	362	353	320	249	415	1431	1131,1	440,2	1598,5	814,3	2758,1	1051	111	152	161	85	117	58	123
Zr	60	120	130	90	200	110	91,6	153,1	55,8	121,8	80,1	70,9	66,1	60	70	80	130	90	70	80
Y	7,8	4,6	4,9	3,8	8	8,8	13,1	27,6	19,8	6,5	16,6	5,5	13,6	15,8	21,5	21,2	12,4	21,1	14,5	21,1
La	16,4	8,8	10	7,5	11,2	9,8	15,3	17,5	2,2	11,3	15,8	6,4	12,4	10,6	11,6	14,6	7	13,9	12	12,8
Ce	27,9	14,6	15,5	12,1	19,4	16	27,4	35,4	6,8	18,3	30,4	10,8	21,8	21,7	25,1	31,2	14,8	28,5	22,9	27,5
Pr	2,26	1,28	1,4	1,12	1,94	1,66	2,92	4,23	1,14	1,78	3,34	1,17	2,31	2,6	3,22	3,78	1,78	3,39	2,67	3,48
Nd	6,4	4	4,2	3,5	6,5	5,8	10,2	16,5	6,1	6,5	14	4,2	8,5	9,9	12,3	14	6,8	12,6	9,7	13,4
Sm	1,01	0,63	0,72	0,64	1,19	1,22	1,92	3,82	1,89	1,13	2,64	0,85	1,93	2,3	3,02	3,11	1,73	2,97	2,13	3,17
Eu	0,33	0,45	0,47	0,52	0,69	0,62	0,37	0,82	0,74	0,61	0,68	0,43	0,61	0,69	0,88	0,92	0,39	0,81	0,73	0,88
Gd	1,01	0,7	0,71	0,63	1,27	1,44	1,98	4,14	3,07	1,2	2,79	0,95	2,23	2,52	3,42	3,48	1,96	3,33	2,35	3,45
Dy	1,09	0,64	0,69	0,52	1,18	1,42	0,32	0,67	0,51	0,18	0,42	0,14	0,35	0,37	0,5	0,5	0,32	0,5	0,36	0,53
Tb	0,16	0,09	0,1	0,08	0,19	0,21	2,11	4,49	3,56	1,24	2,68	1,05	2,21	2,44	3,37	3,33	2,22	3,27	2,26	3,5
Ho	0,23	0,15	0,15	0,13	0,26	0,31	0,47	0,95	0,68	0,24	0,54	0,21	0,48	0,52	0,72	0,71	0,47	0,71	0,48	0,73
Er	0,82	0,5	0,52	0,43	0,87	0,96	1,43	2,93	2,18	0,82	1,66	0,75	1,52	1,62	2,26	2,27	1,59	2,26	1,54	2,27
Tm	0,15	0,09	0,11	0,08	0,15	0,16	0,21	0,44	0,33	0,12	0,27	0,09	0,22	0,26	0,35	0,35	0,26	0,36	0,24	0,36
Yb	0,98	0,58	0,63	0,47	0,94	0,94	1,44	2,99	1,91	0,85	1,82	0,74	1,48	1,52	2,19	2,13	1,56	2,13	1,51	2,29
Lu	0,16	0,11	0,12	0,08	0,17	0,15	0,26	0,49	0,31	0,15	0,29	0,11	0,25	0,25	0,35	0,35	0,25	0,34	0,24	0,37
Mg#	23,2	26,2	39,2	44,6	37,2	42,4	45,0	33,6	66,8	41,2	49,5	42,3	43,6	53,3	36,7	47,5	54,0	44,2	54,5	42,14
(La/Yb)N	12,00	10,88	11,39	11,45	8,55	7,48	7,62	4,20	0,83	9,54	6,23	6,20	6,01	5,00	3,80	4,92	3,22	4,68	5,70	4,01
(La/Sm)N	10,48	9,02	8,97	7,57	6,08	5,19	5,14	2,96	0,75	6,46	3,86	4,86	4,15	2,98	2,48	3,03	2,61	3,02	3,64	2,61
(Gd/Yb)N	0,85	1,00	0,93	1,11	1,12	1,27	1,14	1,15	1,33	1,17	1,27	1,06	1,25	1,37	1,29	1,35	1,04	1,29	1,29	1,25
Eu*	5,70	3,75	4,03	3,58	6,93	7,47	11,00	22,43	13,58	6,57	15,31	5,07	11,70	13,58	18,12	18,55	10,38	17,74	12,62	18,65
Eu/Eu*	1,00	2,07	2,01	2,50	1,72	1,43	0,58	0,63	0,94	1,60	0,77	1,46	0,90	0,88	0,84	0,85	0,65	0,79	1,00	0,81

APPENDIX 2:
Methods Used

1. **Geological Map**

1/25000 scale geological map of Kavacık granite was drawn with the fieldworks. Contact relationships and expansion of granite in Bornova complex has been determined. Field observations made along cross-section lines in land, strike-dip measurements, systematic samples taken and thin sections of these samples were examined under a microscope. Thus, petrographical analyses of granite were made.

2. **Petrography**

Thin sections were prepared in the Thin Secion and Gemology Laboratory in Dokuz Eylul University Department Of Geological Engineering. Plane surfaces were obtained with the help of a rotary disk from the samples taken from the land, the samples adherend to slide were cut 0.3 mm thin with thin section tool. After adhesion to slide, the sections were made suitable for examination in thin section tool with the help of suitable adhesives and pressure.

3. **Geochemistry**

Geochemical analyses and absolute age analyses of samples, taken from land, were made. Major oxide, trace element, rare earth elements (REE) values obtained by geochemical analyses were evaluated by using Minpet program and graphics of nomenclature, classification and formation environments were drawn and evaluated.

4. **Geochronology**

Zircon (U/Pb) were used to absolute dating of Kavacık granite. Zircon separation and analysis process from samples, taken from the land, were made in Dokuz Eylül University at Geological Engineering Sample Preparation Laboratory.

Mineral (Zirkon) Enrichment

Zircon mineral has been separated from the relevant samples for use in the radiogenic dating planned to be made within the scope of the project. Approximately 7-10 kg samples were taken from the samples of Kavacık granite, the required mineral enrichment process were made in 'Sample Preparation Laboratory'. For this purpose, the mineral separation of the samples, taken from the land, for geochronology studies and purification of minerals to be analyzed were carried out. Details of the process sequence for mineral separation are given in the following diagram (Figure 2).

Jaw Crusher

The samples, taken from the land, are cleaned before being crushed in the jaw crusher and made suitable sizes with tools such as sledgehammer. Suitable sample sizes are 10-15 cm in size grinded up to make 2-3 cm size in jaw crusher. The samples that become to the desired size are divided into groups of 400-500 gr by the quartering method.

Sieving

Since the samples crushed in the jaw crusher are heterogeneous, they are divided into four different group by electric sieve in sizes of 63-12 μm, 125-180 μm, 180-225 μm and <225 μm.

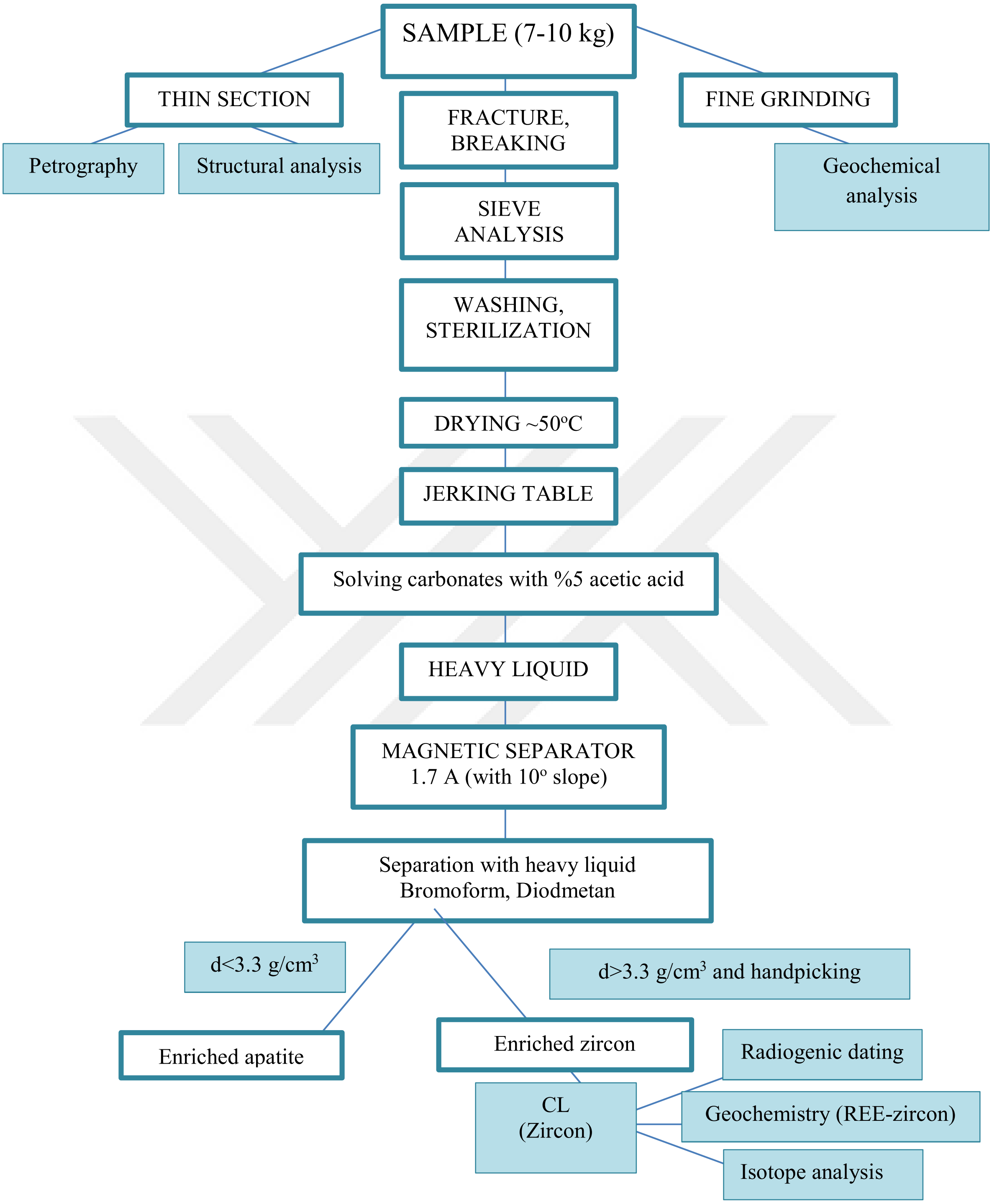

Figure A.1 Diagram of separation of zircon minerals observed in samples made in Kavacık granite

CL Images and ICP-MS LA Analytical Method

The distinguished zircon grains were selected with the help of a stereomicroscope and put into the epoxy in the appropriate mechanism, making them suitable for both CL and ICP-MS LA analyzes. Cathodoluminescence (CL) images were obtained in Earth Sciences Institute of Mainz University (Germany) with the help of a Jeol JXA-8900RL electron microscope. In the same department, U, Th and PB isotope measurements were performed with the ESINWR193 ArF laser system, which is capable of producing 193 nm wavelength laser paired with Agilent 7500ce quadrupole ICP-MS. The first data obtained is calculated by GLITTER 4.4.1 program and it is made suitable to the table to be created in excel. Concordia diagrams are drawn in the ISOPLOT program as the result of analytical calculations made in Excel.

Zircon Mineral Separation for U-Pb

The grains, which are sized by sieve analysis, are purified by washing with national quartz and distilled water. The washed and purified samples are put on to dry in a centrifuge at 50 ° C for 24 hours. Drying samples are separated from each other by using density differences with shaking table. The highest minerals are collected in the vessel in farthest point of the shaky table, the minerals collected uppermost that can be easily carried on the surface of water are the lightest minerals. In order to separate the zircons from the heavy grains collected, firstly the carbonates are dissolved with 5% acetic acid. Grains that purified from carbonate are separated by heavy liquid method. Diiodmethane was used as heavy liquid in Dokuz Eylül University Sample Preparation Laboratory. In the heavy liquid method, in the sample emptied into the heavy liquid, grains such as zircon, which is heavier than the liquid in density, minerals such as light quartz, feldspar group minerals remain on the surface of the liquid. The minerals, sink to the bottom, in the heavy liquid are cleaned with acetone after being filtered on filter paper.

The zircon grains obtained to this stage are separated and enriched. Finally, the zircon grains are selected with a needle under a binocular microscope.

Zircon grinds of Kavacık granite has been sent to Mainz Johannes Gutenberg University Mineral Laboratory to radiogenic dating.

5. Petrographic analysis

Rocks in the study area were examined in land as macroscopic dimension as to color, fabric, forms existing in the nature to be able to reveal petrographic properties. These macroscopic sized samples, taken from the observation points, were examined under a underlighted polarizing microscope with thin sections prepared for interpretation on the microscopic scale. After these studies, mineral compositions, micro fabrics, alteration properties and petrographic properties of the rocks were revealed.

6. Structural analysis

Structural analyzes are used to determine the structural properties of the rocks in land works. These analyzes are geometric, kinematic and dynamic analyzes, respectively.

In order to determine the structural properties of Kavacık granite and surrounding rocks, coordinates were taken at 130 different observation points, strike and dip measurements of the rocks were made with the help of compass and directional samples were taken. The mesoscopic and microscopic scale structural elements in the tectonic slices forming the Bornova complex and the kinematic properties of these structures are described. The obtained data were interpreted in contour diagrams using stereographic projection methods.

KAVACIK GRANİTİ'NİN
JEOLOJI HARITASI ve ENİNE KESİTLERİ